A GENERAL INVESTIGATION OF HYPERSONIC STABILITY AND CONTROL UNDER TRIMMED FLIGHT CONDITIONS

(Second Quarterly Technical Report)

Prepared under Bureau of Naval Weapons

Contract NOw 64-0201-c

FLIGHT SCIENCES LABORATORY, Inc.
Buffalo, New York

R-63-011-109
24 June 1964

SUMMARY

Analytic equations were determined for the force and moment coefficients and stability derivatives of various shapes in Newtonian flow. These results follow from an application of the general method presented in the "First Quarterly Technical Report".

Equations for all the important damping derivatives of the cone at zero sideslip and roll have been determined as a function of angle of attack. The constants in these simple equations can be determined numerically for any C.G. location and any cone angle. For slender cones, with certain restrictions on the C.G. location, the constants in the stability derivative equations have also been determined analytically. Similar results have been obtained for the delta planform with diamond shape cross-section perpendicular to the longitudinal axis. A preliminary investigation has also been conducted on the elliptic cone, and equations have been established for the longitudinal force coefficients.

A preliminary investigation has been made of the effects of bluntness on the constants in the stability equations. These results have been applied to the determination of analytic equations for the longitudinal force coefficients of the blunt cone.

An initial investigation has been undertaken into other hypersonic theories, besides Newtonian, for predicting surface pressures. This investigation is continuing. Based on these preliminary results, a method has been outlined for determining the variations of the hypersonic stability derivatives with Mach number. The method will be checked against experimental results during the next quarter.

TABLE OF CONTENTS

TABLE OF CONTENTS (Cont)

LIST OF FIGURES

TABLE OF SYMBOLS

All symbols not shown here are defined in the "First Quarterly Technical Report".

A_B Base area of the bottom half of a spherical cap segment.

C_p Pressure coefficient

e Ratio of horizontal to vertical axes of a cone of elliptic cross-section

f_B Bluntness factor defined in Eq. (5.4)

K Pressure coefficient constant

M Mach number

R Radius of spherical cap

R_B Radius of the base of a spherical cap segment

R_c Radius of the base of a cone

S_B Planform area of a spherical cap segment

S_c Planform area of a truncated cone

β $= \sqrt{M^2-1}$
Also angle of sideslip

γ Gas constant

δ Angle between the free stream flow and the plane tangent to the surface at a point. Also compression angle

δ_e Expansion angle

Λ Leading edge sweep angle

Subscripts

B Refers to the bottom half of a body
Also the blunted portion of a body

C Refers to the cone portion of a body

BC Refers to a blunted cone body

T Refers to the top half of a body

1.0 Introduction

Much of the basic groundwork for the application of simple Newtonian theory to the determination of the forces and moments, and stability derivatives of various wing and body shapes is presented in the "First Quarterly Technical Report". It has been demonstrated there that reasonably simple analytic equations are possible for all the important aerodynamic stability derivatives as a function of angle of attack.

In the "First Quarterly Technical Report", the methods developed were applied to the cone. Only the static forces and moments, and the static derivatives were determined during the first quarter. During this second quarter, the methods have been applied to the determination of the important damping derivatives of the cone, and the results are included in this report.

Several other shapes have been looked at in the same detail. Analytic expressions have been derived for the force and moment coefficients and stability derivatives (both static and dynamic) of the delta planform with diamond shape cross-section. Similar results have been obtained for the segment of a spherical cap. One of the objectives has been to apply the spherical cap results to the determination of the stability derivatives of a blunt cone. Some work has also been done on the determination of static forces and moments and their derivatives for the delta planform with elliptic cross-section.

Several methods are outlined for the determination of analytic equations for the longitudinal force coefficients of blunted surfaces. These methods have been applied to the blunt cone. The use of blunt bodies in the hypersonic region is often mandatory, and the stability derivatives of such surfaces are therefore of special interest.

Pressure distributions computed using simple Newtonian theory are generally applicable only for a limited class of aerodynamic shapes and limited Mach number and surface angles of attack ($M\delta > 4.0$). A beginning has been made into an investigation of other hypersonic theories for computing surface pressures. The purpose is to extend the methods developed for computing Newtonian stability derivatives to lower Mach numbers and angles of attack.

Throughout this report reference will be made to equations, sections, and figures in the "First Quarterly Technical Report". An equation, section or figure number followed by the letter F refers to the equation, section, or figure in the "First Quarterly Technical Report".

2.0 Analytic Equations - The Circular Cone

2.1 General Discussion

The general methods developed for determining analytic equations for the stability derivatives were applied to the cone in the "First Quarterly Technical Report". During the first quarter, only the static coefficients and static derivatives had been determined. The damping derivatives have since been evaluated and are presented in this report.

At the outset, it should be stated that the stability derivatives are computed under the special conditions of zero roll ($\phi = 0$) and zero sideslip ($\beta = 0$) of the body. The analytic equations derived for the damping derivatives are therefore a function of only angle of attack for a given body shape. For the present, the derivatives are computed assuming simple Newtonian theory. A preliminary consideration of Mach number effects is discussed in Section 6.0.

For each damping derivative, the damping of a half body with flat side up at positive angles of attack is first determined. These results are then generalized to apply to full bodies at all angles of attack.

2.2 Damping in Pitch - C_{m_q}

As shown in Section 6.1F, the equation of a cone in rectangular coordinates can be expressed as

$$F(x, y, z) = (\tan^2\theta)\, x^2 - y^2 - z^2 = 0 \qquad (6.1F)$$

The axes system used, and the positive direction of forces, moments, and angular rotations are indicated on Figure (1.0F)

As shown in Section 5.2F, the damping in pitch of any body can be expressed in one of two ways

$$C_{m_q} = (K_{mq})_1 \cos\alpha + (K_{mq})_2 \sin\alpha \qquad (5.17F)$$

$$C_{m_q} = m_q \sin(\theta_{mq} + \alpha) \qquad (5.18F)$$

The constants $(K_{mq})_1$ and $(K_{mq})_2$ are determined from Eqs. (5.15F) and (5.16F) by integrating over the body surface. The partial derivatives appearing in these equations are determined from the equation of the surface, Eq. (6.1F). The constants m_q and θ_{mq} in Eq. (5.18F) are defined by Eqs. (5.19F) and (5.20F), and are repeated here for convenience.

$$m_q = \sqrt{(K_{mq})_1^2 + (K_{mq})_2^2} \qquad (5.19F)$$

$$\theta_{mq} = \tan^{-1}\frac{(K_{mq})_1}{(K_{mq})_2} = \sin^{-1}\frac{(K_{mq})_1}{\sqrt{(K_{mq})_1^2 + (K_{mq})_2^2}} \qquad (5.20F)$$

The constants $(K_{mq})_1$ and $(K_{mq})_2$ have been determined for a half circular cone with flat side up under the assumption that the angle of attack is positive so that the complete bottom always "sees" the flow.

$$(K_{mq})_1 = -\pi\left[1 - \frac{8}{3}\left(\frac{x_0}{C}\right) + 2\left(\frac{x_0}{C}\right)^2\right]\tan\theta - \frac{32}{3}\left(\frac{z_0}{C}\right)\left[1 - \frac{3}{2}\left(\frac{x_0}{C}\right)\right]\sin^2\theta -$$

$$-\pi\left[1 - 2\left(\frac{x_0}{C}\right)^2 + 4\left(\frac{z_0}{C}\right)^2\right]\tan\theta\sin^2\theta - \frac{32}{3}\left(\frac{z_0}{C}\right)\tan^2\theta\sin^2\theta -$$

$$-\pi\tan^3\theta\sin^2\theta \qquad (2.1)$$

$$(K_{mq})_2 = -\frac{8}{3}\left[1-\frac{8}{3}\left(\frac{x_o}{c}\right)+2\left(\frac{x_o}{c}\right)^2\right]-\frac{8}{3}\pi\left(\frac{z_o}{c}\right)\left[1-\frac{3}{2}\left(\frac{x_o}{c}\right)\right]\tan\theta -$$

$$-\frac{8}{3}\left[1-2\left(\frac{x_o}{c}\right)^2+3\left(\frac{z_o}{c}\right)^2\right]\sin^2\theta - 4\pi\left(\frac{x_o}{c}\right)\left(\frac{z_o}{c}\right)\tan\theta\sin^2\theta -$$

$$-\frac{8}{3}\tan^2\theta\sin^2\theta \qquad (2.2)$$

In these expressions, θ is the cone half angle, and x_o and z_o are the horizontal and vertical C.G. location along and perpendicular to the cone axis respectively. The damping in pitch (C_{m_q}) of the half cone is based on the planform area of the cone and the cone length (c). The symbols used here are the same as those in the "First Quarterly Technical Report", and one can refer to this report for definitions of terms.

For any given cone angle (θ) and C.G. location (x_o, z_o) it is possible to evaluate $(K_{mq})_1$ and $(K_{mq})_2$ numerically. The damping in pitch as a function of angle of attack can then be determined from Eq. (5.17F). A more useful expression for the damping in pitch is given by Eq. (5.18F). The constants m_q and θ_{mq} can be evaluated numerically from $(K_{mq})_1$ and $(K_{mq})_2$. It thus becomes evident that as long as all of the conical surface "sees" the flow, it is possible to derive a simple analytic expression for the damping in pitch. It is interesting to note that based on Newtonian theory, all shapes can be cast in the same analytic form, and their relative damping qualities compared.

It would be very useful if m_q and θ_{mq} in Eq. (5.18F) could be evaluated analytically in terms of the geometric parameter of the surface (θ), and the C. G. location (x_o, z_o). Examination of Eqs. (2.1) and (2.2) substituted in Eqs. (5.19F) and (5.20F) indicates that the analytic expressions will be very involved and therefore of little practical use. Considerable simplification is possible if one limits the discussion to cones of small angle. It is then necessary to retain only the first terms in the expressions for $(K_{mq})_1$ and $(K_{mq})_2$. Damping derivatives for small cone angles will be discussed shortly.

It becomes evident from examining Eqs. (2.1) and (2.2) that the damping

in pitch is a rather involved function of C.G. location. No simple relationships can be established for transferring the damping in pitch from one C.G. to another, as is the case for the static derivatives of the surface.

The pitch damping constants in Eqs. (5.18F) for a half cone are plotted as a function of cone half angle and C.G. location, both vertical and horizontal, in Figs. 1, 2, and 3. It becomes evident from the figures that the damping in pitch is an especially strong function of horizontal C. G. The figures indicate that the damping is large about the nose and small about a point 2/3 of the cone length aft of the nose. As long as the C. G. remains in the cone, the damping is not a strong function of vertical C. G. location except at large cone angles and horizontal C. G.'s aft of the 2/3 point. The vertical C. G.'s chosen are rather extreme and represent the limit the C. G. can move vertically and still remain within the envelope of the cone.

It is instructive to look at the damping of a half cone under the assumption that the cone angle is small, and the vertical C.G. location (z_0/c) is also small. This will be true if the C.G. is located inside the cone envelope so that $|z_0/x_0| < \tan\theta$. Retaining up to first order terms of small quantities, Eqs. (2.1) and (2.2) reduce to

$$(K_{m_q})_{\perp} = -\pi\left[1 - \frac{8}{3}\left(\frac{x_0}{c}\right) + 2\left(\frac{x_0}{c}\right)^2\right]\theta \tag{2.3}$$

$$(K_{m_q})_{\parallel} = -\frac{8}{3}\left[1 - \frac{3}{2}\left(\frac{x_0}{c}\right) + 2\left(\frac{x_0}{c}\right)^2\right] \tag{2.4}$$

Substituting in Eqs. (5.19F) and (5.20F) and retaining up to first order terms in θ results in the following:

$$m_q = \frac{8}{3}\left[1 - \frac{3}{2}\left(\frac{x_0}{c}\right) + 2\left(\frac{x_0}{c}\right)^2\right] \tag{2.5}$$

$$\theta_{m_q} = \pi + \theta'_{m_q} \quad , \text{ where } \quad \theta'_{m_q} = \frac{3\pi}{8}\theta \tag{2.6}$$

Thus for a half cone of small semi-angle (θ), the damping in pitch equation, Eq. (5.18F), is

$$C_{m_q} = -\frac{8}{3}\left[1 - \frac{8}{3}\left(\frac{x_o}{c}\right) + 2\left(\frac{x_o}{c}\right)^2\right] \sin\left(\frac{3\pi}{8}\theta + \alpha\right) \qquad (2.7)$$

It is interesting to note that the damping in pitch of a slender cone is only a function of longitudinal C. G. location. Eqs. (2.5) and (2.6) should be compared to the exact results of Figs. 1, 2, and 3. Eq. (2.7) will give reasonably good results up to cone angles of about 8 degrees. It is possible to derive m_q and θ_{mq} with higher order terms in small quantities. This will increase the range of validity of the pitch damping equation and also show the effects of vertical C. G. location.

Eq. (2.7) indicates the strong effect of longitudinal C. G. location on the damping in pitch of a cone. Eqs. (2.3), (2.4), (2.5), and (2.6) are plotted as a function of longitudinal C. G. position in Fig. 4. It becomes obvious that the damping varies widely with C. G., and is a maximum for the C. G. at the nose and a minimum for the C. G. at 2/3 of the cone length aft of the nose.

Up to now, the discussion has been concerned with the damping in pitch of a half cone with flat side up at positive angles of attack. The derivation of analytic expressions for the damping in pitch of a complete cone at all angles of attack will now be discussed in some detail.

In order to determine the damping in pitch of the top half of the cone, it is necessary to evaluate the constants $(K_{mq})_1$ and $(K_{mq})_2$ of Eq. (5.17F) for the top half. This may be done following the integration procedure outlined in Section 5.2F . The method is the same one used for the bottom, only the limits of integration are different. These constants will be valid at negative angles of attack for a half cone with flat side down. Following this procedure, the constants for the top of the cone become

$$(K_{mq})_1 = -\pi\left[1-\frac{8}{3}\left(\frac{x_o}{c}\right)+2\left(\frac{x_o}{c}\right)^2\right]\tan\theta+\frac{32}{3}\left(\frac{z_o}{c}\right)\left[1-\frac{3}{2}\left(\frac{x_o}{c}\right)\right]\sin^2\theta-$$

$$-\pi\left[1-2\left(\frac{x_o}{c}\right)^2+4\left(\frac{z_o}{c}\right)^2\right]\tan\theta\sin^2\theta+\frac{32}{3}\left(\frac{z_o}{c}\right)\tan^2\theta\sin^2\theta-$$

$$-\pi\tan^3\theta\sin^2\theta \qquad (2.8)$$

$$(K_{mq})_2 = \frac{8}{3}\left[1-\frac{8}{3}\left(\frac{x_o}{c}\right)+2\left(\frac{x_o}{c}\right)^2\right]-\frac{8}{3}\pi\left(\frac{z_o}{c}\right)\left[1-\frac{3}{2}\left(\frac{x_o}{c}\right)\right]\tan\theta+$$

$$+\frac{8}{3}\left[1-2\left(\frac{x_o}{c}\right)^2+3\left(\frac{z_o}{c}\right)^2\right]\sin^2\theta-4\pi\left(\frac{x_o}{c}\right)\left(\frac{z_o}{c}\right)\tan\theta\sin^2\theta+$$

$$+\frac{8}{3}\tan^2\theta\sin^2\theta \qquad (2.9)$$

These constants are identical to those for the bottom half of the cone, except for some important differences in signs of the various terms. Inspection shows that $(K_{mq})_1$ for the top can be obtained from $(K_{mq})_1$ for the bottom by substitution $-z_o$ for z_o. The second constant, $(K_{mq})_2$ of the top can be obtained from $(K_{mq})_2$ of the bottom by first substituting $-z_o$ for z_o, and then changing the sign of every term.

The constants m_q and θ_{mq} for the top are obtained by substituting $(K_{mq})_1$ and $(K_{mq})_2$ in Eqs. (5.19F) and (5.20F). As long as the top and bottom of the cone completely see the flow, the damping in pitch of the full cone can be written as

$$C_{m_q} = (C_{m_q})_B + (C_{m_q})_T$$

$$= (m_q)_B \sin(\theta_{mq_B}+\alpha) + (m_q)_T \sin(\theta_{mq_T}+\alpha) \qquad (2.10)$$

The subscripts B and T refer to the bottom and top of the cone respectively.

The θ_{mq_B} and θ_{mq_T} shown in Eq. (2.10) are not in general acute angles as determined from Eq. (5.20F). Methods of obtaining the acute angle form are discussed in some detail in Section 5.2F. In general, for the bottom half of the cone, $(K_{mq})_1$ and $(K_{mq})_2$ are both negative. For the top half of the cone, it follows from the previous discussion that in general $(K_{mq})_1$ is negative and $(K_{mq})_2$ is positive. Under these conditions it becomes apparent that θ_{mq_B} is in the third quadrant, and θ_{mq_T} is in the fourth quadrant. In terms of acute angles, the angles for the bottom and top can then be written as

$$\theta_{mq_B} = \pi + \theta'_{mq_B}$$

$$\theta_{mq_T} = 2\pi - \theta'_{mq_T}$$

where the primed values are acute angles. By substituting in Eq. (2.10), the damping in pitch of the full cone becomes

$$C_{mq} = -(m_q)_B \sin(\theta'_{mq_B} + \alpha) - (m_q)_T \sin(\theta'_{mq_T} - \alpha) \qquad (2.11)$$

It should be of interest to note that Eqs. (2.10) and (2.11) will apply whether or not the top and bottom surface are of the same shape. It is

only necessary that the constants for the top shape and bottom shape be computed separately.

If the C.G. is located in the horizontal plane of symmetry of the cone ($z_o = 0$), then the damping of the complete cone assumes an especially simple form since

$$(m_q)_B = (m_q)_T = m_q$$

$$\theta'_{mq_B} = \theta'_{mq_T} = \theta'_{mq}$$

Eq. (2.11) now becomes

$$C_{m_q} = - m_q \left[\sin (\theta'_{mq} + \alpha) + \sin (\theta'_{mq} - \alpha) \right] \qquad (2.12)$$

This equation could have been arrived at from simple physical reasoning since it says that the pitch damping of the top of the cone at negative angles of attack is no different than the damping of the bottom at positive angles of attack if the C.G. is in the horizontal plane of symmetry.

The first and second terms of Eq. (2.12) apply to lower and upper surface respectively. The maximum positive and negative angle of attack for which this equation is exactly true is determined as the minimum positive and negative angles of attack for which the normal component of free stream is always inward at any point on the complete cone surface. For the damping in pitch, this can be determined from Eq. (5.12F) for the condition $(\vec{v} \cdot \vec{p}) > 0$. But this condition is no different than that for the static forces and moments and their derivatives as determined from Eq. (3.12F). When Eq. (3.12F) is applied to the complete cone, the angle of attack range for which Eq. (2.12) is exactly valid is $-\theta \leq \alpha \leq \theta$.

It will now prove instructive to examine Eq. (2.12) in terms of a

specific example and determine the relative magnitude of the two terms at angles of attack. If one selects as an example a 5 degree cone, Eq. (2.12) is exactly valid for the angle of attack range $-5^0 \leq \alpha \leq 5^0$. Also for a 5^0 cone it is sufficiently accurate to use the small cone angle form of the pitch damping constants, Eq. (2.5) and (2.6). Eq. (2.12) now becomes

$$C_{m_q} = -\frac{8}{3}\left[1-\frac{8}{3}\left(\frac{x_0}{c}\right)+2\left(\frac{x_0}{c}\right)^2\right]\left[\sin\left(\frac{3\pi}{8}\theta+\alpha\right)+\sin\left(\frac{3\pi}{8}\theta-\alpha\right)\right] \qquad (2.13)$$

At plus 5^0 angle of attack Eq. (2.13) is still valid for a 5^0 semi-angle cone, and the relative magnitude of the contribution of the top and bottom to the damping can be determined from the following ratio.

$$\frac{\sin\left(\frac{3\pi}{8}\theta-\alpha\right)}{\sin\left(\frac{3\pi}{8}\theta+\alpha\right)} = \frac{\sin(5.90^\circ-5^\circ)}{\sin(5.90^\circ+5^\circ)} = \frac{\sin(.90^\circ)}{\sin(10.90^\circ)} = .0825$$

Thus at 5^0 angle of attack the contribution of the top of the cone is only about 8 percent of the bottom. At 5^0 negative angle of attack just the reverse is true, the bottom is only 8 percent of the top.

Obviously only a maximum of 8 percent error is introducted if the contribution of the top is neglected after 5 degrees angle of attack and the bottom is neglected after angles of attack less than -5^0. The error will be considerably less if the top and bottom terms are retained until the angles of attack are equal to the absolute value of the "effective" surface angle $\frac{3\pi}{8}\theta$. For the 5^0 cone this effective angle is 5.90 degrees. These same arguments hold for even larger cone angles and a wider variety of shapes than the simple cone. On the basis of these and similar results it is possible to write reasonably accurate results for the damping in pitch throughout the angle of attack range from Eq. (2.12) by dropping appropriate terms. We can thus write,

$\alpha \leq -\theta'_{m_q}$

$$C_{m_q} = -m_q \sin(\theta'_{m_q} - \alpha) \qquad (2.14)$$

$-\theta'_{mq} \leq \alpha \leq \theta'_{mq}$

$$C_{m_q} = -m_q \left[\sin(\theta'_{mq} + \alpha) + \sin(\theta'_{mq} - \alpha) \right] \tag{2.15}$$

$\alpha \geq \theta'_{mq}$

$$C_{m_q} = -m_q \sin(\theta'_{mq} + \alpha) \tag{2.16}$$

For any full cone, the constants in Eqs. (2.14), (2.15), and (2.16) can be determined numerically as discussed previously. For a slender cone the analytic forms of the constants are especially simple and the damping of a full slender cone throughout the angle of attack range can be written as follows:

$\alpha \leq -\frac{3\pi}{8}\theta$

$$C_{m_q} = -\frac{\theta}{3}\left[1 - \frac{8}{3}\left(\frac{x_o}{c}\right) + 2\left(\frac{x_o}{c}\right)^2\right] \sin\left(\frac{3\pi}{8}\theta - \alpha\right) \tag{2.17}$$

$-\frac{3\pi}{8}\theta \leq \alpha \leq \frac{3\pi}{8}\theta$

$$C_{m_q} = -\frac{8}{3}\left[1 - \frac{8}{3}\left(\frac{x_o}{c}\right) + 2\left(\frac{x_o}{c}\right)^2\right]\left[\sin\left(\frac{3\pi}{8}\theta + \alpha\right) + \sin\left(\frac{3\pi}{8}\theta - \alpha\right)\right] \tag{2.18}$$

$\alpha \geq \frac{3\pi}{8}\theta$

$$C_{m_q} = -\frac{8}{3}\left[1 - \frac{8}{3}\left(\frac{x_o}{c}\right) + 2\left(\frac{x_o}{c}\right)^2\right] \sin\left(\frac{3\pi}{8}\theta + \alpha\right) \tag{2.19}$$

The damping in pitch at zero angle of attack for a slender cone becomes from Eq. (2.18),

$$C_{m_q} = -2\pi\left[1 - \frac{8}{3}\left(\frac{x_o}{c}\right) + 2\left(\frac{x_o}{c}\right)^2\right]\theta \tag{2.20}$$

If the C.G. is not located in the horizontal plane of symmetry ($z_o \neq 0$),

then the constants for the top and bottom of the cone are not identical and the more general form of the damping in pitch equation of the complete cone, Eq. (2.11), must be used. The constants for the top and bottom must then be evaluated separately. From Eq. (2.11), good approximate expressions for the damping in pitch throughout the angle of attack range can be derived using the same procedure that was used for the slender cone. From Eq. (2.11), these equations become

$\alpha \leq -\theta'_{mq_B}$

$$C_{m_q} = -(m_q)_T \sin(\theta'_{mq_T} - \alpha) \tag{2.21}$$

$-\theta'_{mq_B} \leq \alpha \leq \theta'_{mq_T}$

$$C_{m_q} = -(m_q)_B \sin(\theta'_{mq_B} + \alpha) - (m_q)_T \sin(\theta'_{mq_T} - \alpha) \tag{2.22}$$

$\alpha \geq \theta'_{mq_T}$

$$C_{m_q} = -(m_q)_B \sin(\theta'_{mq_B} + \alpha) \tag{2.23}$$

Although the discussion here has been concerned with the full cone, the form of the results will be the same for any shape surface in Newtonian flow. In fact, the upper and lower surface need not be the same shape for Eqs. (2.21), (2.22), and (2.23) to be applicable. It is only necessary that the constants in these equations be determined separately for the top and bottom shape. Similar results for the damping in pitch have been determined for other shapes and these will be presented in subsequent sections.

The other damping derivatives can be determined following essentially the same procedure, and these will be discussed in the sections that follow.

2.3 Damping in Yaw - C_{n_r}

It is demonstrated in Section 5.3F that the damping in yaw of an aerodynamic shape can be expressed as

$$C_{n_r} = (K_{nr})_1 \cos\alpha + (K_{nr})_2 \sin\alpha \qquad (5.28F)$$

$$C_{n_r} = m_{nr} \sin(\theta_{nr} + \alpha) \qquad (5.31F)$$

where

$$m_{nr} = \sqrt{(K_{nr})_1^2 + (K_{nr})_2^2} \qquad (5.32F)$$

$$\theta_{nr} = \tan^{-1}\frac{(K_{nr})_1}{(K_{nr})_2} = \sin^{-1}\frac{(K_{nr})_1}{\sqrt{(K_{nr})_1^2 + (K_{nr})_2^2}} \qquad (5.33F)$$

The constants $(K_{nr})_1$ and $(K_{nr})_2$ are determined from Eqs. (5.29F), and (5.30F) using the equation of the surface, Eq. (6.1F).

For a half cone with flat side up at positive angles of attack, the following expressions for the constants have been evaluated.

$$(K_{nr})_1 = -\pi\left[1 - \frac{8}{3}\left(\frac{x_o}{c}\right) + 2\left(\frac{x_o}{c}\right)^2\right]\tan\theta -$$

$$-\pi\left[1 - 2\left(\frac{x_o}{c}\right)^2 + 4\left(\frac{y_o}{c}\right)^2\right]\tan\theta\sin^2\theta - \pi\tan^3\theta\sin^2\theta \qquad (2.24)$$

$$(K_{nr})_2 = -\frac{4}{3}\left[1 - \frac{8}{3}\left(\frac{x_o}{c}\right) + 2\left(\frac{x_o}{c}\right)^2\right] - \frac{4}{3}\left[1 - 2\left(\frac{x_o}{c}\right)^2 + 6\left(\frac{y_o}{c}\right)^2\right]\sin^2\theta -$$

$$-\frac{4}{3}\tan^2\theta\sin^2\theta \qquad (2.25)$$

For any cone half angle (θ) and C.G. location (x_o, y_o), it is possible to evaluate numerically $(K_{nr})_1$ and $(K_{nr})_2$, and also the constants m_{nr} and θ_{nr}. Eqs. (5.28F) and (5.31F) will then give the damping in yaw as a function of angle of attack for positive angles of attack.

The damping in yaw is a function of both longitudinal and lateral C.G. location. No simple C.G. transfer relationships can be derived as they were for the static derivatives.

The yaw damping constants in Eq. (5.31F), with the acute angle form for θ_{nr} , are plotted for a half cone as a function of cone angle and C.G. location in Figs. 5, 6, and 7. The yaw damping is an especially strong function of longitudinal C. G. position and varies little with lateral C. G. location for moderate cone angles, $\theta < 15^0$. The damping is large about the nose and small about a point 2/3 of the cone length from the nose. Only lateral C. G. locations that lie within the cone envelope have been considered in these figures, $|y_0/x_0| < \tan\theta$.

It is interesting to look at the damping in yaw under the assumption that the cone half angle is small, and the lateral C. G. location is small, $|y_0/x_0| < \tan\theta$. Retaining only up to first order terms in small quantities, the constants can be written as

$$(K_{nr})_1 = -\pi\left[1 - \frac{8}{3}\left(\frac{x_0}{c}\right) + 2\left(\frac{x_0}{c}\right)^2\right]\theta \tag{2.26}$$

$$(K_{nr})_2 = -\frac{4}{3}\left[1 - \frac{8}{3}\left(\frac{x_0}{c}\right) + 2\left(\frac{x_0}{c}\right)^2\right] \tag{2.27}$$

$$m_{nr} = \frac{4}{3}\left[1 - \frac{8}{3}\left(\frac{x_0}{c}\right) + 2\left(\frac{x_0}{c}\right)^2\right] \tag{2.28}$$

$$\theta_{nr} = \pi + \theta'_{nr}\,, \qquad \text{where } \theta'_{nr} = \frac{3\pi}{4}\theta \tag{2.29}$$

For sufficiently small cone angles, Eq. (5.31F) thus becomes

$$C_{n_r} = -\frac{4}{3}\left[1 - \frac{8}{3}\left(\frac{x_0}{c}\right) + 2\left(\frac{x_0}{c}\right)^2\right]\sin\left(\frac{3\pi}{4}\theta + \alpha\right) \tag{2.30}$$

Eqs. (2.28) and (2.29) should be compared to the exact solutions of Figs. 5, 6, and 7. These comparisons indicate that Eq. (2.30) will give reasonably good

results for cone semi-angles less than about 10 degrees. The strong effect of longitudinal C. G. location on the damping in yaw is indicated by the plot of Eqs. (2.26) through (2.29) in Fig. 8. The figure indicates that the damping in yaw is a minimum for the C.G. located at 2/3 of the cone length from the nose.

The damping in yaw of the full cone is now fairly easy to evaluate for all angles of attack. If the constants $(K_{nr})_1$ and $(K_{nr})_2$ for the top half of the full cone are determined, it will be found that the $(K_{nr})_1$ of the top and bottom half are the same, and the $(K_{nr})_2$ of the top is opposite in sign to the $(K_{nr})_2$ of the bottom. This same relationship existed for the $(K_{mq})_1$ and $(K_{mq})_2$ of the top and bottom with the C.G. in the horizontal plane of symmetry. It therefore follows that the damping in yaw for the complete cone is analogous to Eq. (2.12) and can be written as

$$C_{n_r} = -m_{nr}\left[\sin(\theta'_{nr}+\alpha) + \sin(\theta'_{nr}-\alpha)\right] \tag{2.31}$$

The damping in yaw throughout the angle of attack range can now be determined by simple analogy to the damping in pitch equations.

$\underline{\alpha \le -\theta'_{nr}}$

$$C_{n_r} = -m_{nr}\sin(\theta'_{nr}-\alpha) \tag{2.32}$$

$\underline{-\theta'_{nr} \le \alpha \le \theta'_{nr}}$

$$C_{n_r} = -m_{nr}\left[\sin(\theta'_{nr}+\alpha) + \sin(\theta'_{nr}-\alpha)\right] \tag{2.33}$$

$\underline{\alpha \ge \theta'_{nr}}$

$$C_{n_r} = -m_{nr}\sin(\theta'_{nr}+\alpha) \tag{2.34}$$

If the upper and lower surface are not of the same shape, then the constants for the upper and lower surface must be determined separately as indicated in Section 2.2 when discussing the damping in pitch. In such a case, the yaw damping equations will be analogous to the pitch damping Eqs. (2.21), (2.22), and (2.23), and they can be written as follows:

$\alpha \leq -\theta'_{nr_B}$

$$C_{n_r} = -m_{nr_T} \sin(\theta'_{nr_T} - \alpha) \tag{2.35}$$

$-\theta'_{nr_B} \leq \alpha \leq \theta'_{nr_T}$

$$C_{n_r} = -m_{nr_B} \sin(\theta'_{nr_B} + \alpha) - m_{nr_T} \sin(\theta'_{nr_T} - \alpha) \tag{2.36}$$

$\alpha \geq \theta'_{nr_T}$

$$C_{n_r} = -m_{nr_B} \sin(\theta'_{nr_B} + \alpha) \tag{2.37}$$

The subscripts T and B refer to the constants for the top and bottom surface shape respectively.

For a full slender cone Eqs. (2.32), (2.33), and (2.34) assume an especially simple form.

$\alpha \leq -\frac{3\pi}{4}\theta$

$$C_{n_r} = -\frac{4}{3}\left[1 - \frac{8}{3}\left(\frac{x_0}{\ell}\right) + 2\left(\frac{x_0}{\ell}\right)^2\right] \sin\left(\frac{3\pi}{4}\theta - \alpha\right) \tag{2.38}$$

$\underline{-\frac{3\pi}{4}\theta \leq \alpha \leq \frac{3\pi}{4}\theta}$

$$C_{n_r} = -\frac{4}{3}\left[1 - \frac{8}{3}\left(\frac{x_o}{c}\right) + 2\left(\frac{x_o}{c}\right)^2\right]\left[\sin\left(\frac{3\pi}{4}\theta + \alpha\right) + \sin\left(\frac{3\pi}{4}\theta - \alpha\right)\right] \quad (2.39)$$

$\underline{\alpha \geq \frac{3\pi}{4}\theta}$

$$C_{n_r} = -\frac{4}{3}\left[1 - \frac{8}{3}\left(\frac{x_o}{c}\right) + 2\left(\frac{x_o}{c}\right)^2\right]\sin\left(\frac{3\pi}{4}\theta + \alpha\right) \quad (2.40)$$

At zero angle of attack, the damping in yaw of a slender cone can be derived from Eq. (2.39). The result is identical to the damping in pitch at zero angle of attack.

$$C_{n_r} = -2\pi\left[1 - \frac{8}{3}\left(\frac{x_o}{c}\right) + 2\left(\frac{x_o}{c}\right)^2\right]\theta \quad (2.41)$$

2.4 Damping in Roll - C_{l_p}

From Section 5.4F the damping in roll of a surface assuming Newtonian flow can be expressed as

$$C_{l_p} = (K_{lp})_1 \cos\alpha + (K_{lp})_2 \sin\alpha \quad (5.43F)$$

$$C_{l_p} = m_{lp} \sin(\theta_{lp} + \alpha) \quad (5.44F)$$

where

$$m_{lp} = \sqrt{(K_{lp})_1^2 + (K_{lp})_2^2} \quad (5.45F)$$

$$\theta_{lp} = \tan^{-1}\frac{(K_{lp})_1}{(K_{lp})_2} = \sin^{-1}\frac{(K_{lp})_1}{\sqrt{(K_{lp})_1^2 + (K_{lp})_2^2}} \quad (5.46F)$$

Using the equation of the surface, the constants $(K_{\ell p})_1$ and $(K_{\ell p})_2$ can be determined as indicated in Section 5.4F. For a half cone with flat side up, at positive angles of attack, these constants become

$$(K_{\ell p})_1 = -2\pi\left[\left(\frac{y_o}{c}\right)^2 + \left(\frac{z_o}{c}\right)^2\right] \sin\theta\cos\theta \tag{2.42}$$

$$(K_{\ell p})_2 = -\frac{8}{3}\left[2\left(\frac{y_o}{c}\right)^2 + \left(\frac{z_o}{c}\right)^2\right] \cos^2\theta \tag{2.43}$$

For any cone angle (θ) and C.G. location (y_o, z_o), the constants can be evaluated numerically, and the damping in roll of a half cone can be determined as a function of angle of attack from Eq. (5.44F). It is interesting to note, that with the C.G. on the cone axis ($y_o = z_o = 0$), the damping in roll is always zero, as one would expect.

For those cases where the lateral displacement of C.G. is zero, $y_o/c = 0$, the constants assume an especially simple form

$$(K_{\ell p})_1 = -2\pi\left(\frac{z_o}{c}\right)^2 \sin\theta\cos\theta$$

$$= -2\pi\left(\frac{z_o}{c}\right)^2 \tan\theta + 2\pi\left(\frac{z_o}{c}\right)^2 \tan\theta \sin^2\theta \tag{2.44}$$

$$(K_{\ell p})_2 = -\frac{8}{3}\left(\frac{z_o}{c}\right)^2 \cos^2\theta$$

$$= -\frac{8}{3}\left(\frac{z_o}{c}\right)^2 + \frac{8}{3}\left(\frac{z_o}{c}\right)^2 \sin^2\theta \tag{2.45}$$

If the further assumption is made that the cone angle is small, and only up to first order terms in θ are retained, then the constants assume the following values:

$$(K_{\ell p})_1 = -2\pi\left(\frac{\bar{z}_o}{c}\right)^2\theta \tag{2.46}$$

$$(K_{\ell p})_2 = -\frac{\theta}{3}\left(\frac{\bar{z}_o}{c}\right)^2 \tag{2.47}$$

$$m_{\ell p} = \frac{\theta}{3}\left(\frac{\bar{z}_o}{c}\right)^2 \tag{2.48}$$

$$\theta_{\ell p} = \pi + \theta'_{\ell p}\ , \qquad \text{where } \theta'_{\ell p} = \frac{3\pi}{4}\theta \tag{2.49}$$

The roll damping constants determined using Eqs. (2.44) and (2.45) are plotted as a function of cone angle in Fig. 9. These results compare quite well for $\theta < 10^0$ to the small angle expressions, Eqs. (2.48) and (2.49).

For a slender half cone, the damping in roll as a function of angle of attack and vertical C.G. position thus becomes

$$C_{\ell_f} = -\frac{\theta}{3}\left(\frac{\bar{z}_o}{c}\right)^2 \sin\left(\frac{3\pi}{4}\theta + \alpha\right) \tag{2.50}$$

The damping in roll of the full cone is easy to determine once the constants, $(K_{\ell p})_1$ and $(K_{\ell p})_2$, for the top half of the cone are evaluated. Analysis shows that these constants can be derived from those for the bottom half by first substituting $-z_o$ for z_o, and then changing the sign of all the terms in $(K_{\ell p})_2$. It will be remembered that the same procedure applied to the damping in pitch constants. By analogy to Eqs. (2.21), (2.22), and (2.23), the damping in roll equations become

$\alpha \leq -\theta'_{\ell\ell_B}$

$$C_{\ell_p} = -m_{\ell\ell_T} \sin(\theta'_{\ell\ell_T} - \alpha) \tag{2.51}$$

$-\theta'_{\ell\ell_B} \leq \alpha \leq \theta'_{\ell\ell_T}$

$$C_{\ell_p} = -m_{\ell\ell_B} \sin(\theta'_{\ell\ell_B} + \alpha) - m_{\ell\ell_T} \sin(\theta'_{\ell\ell_T} - \alpha) \tag{2.52}$$

$\alpha \geq \theta'_{\ell\ell_T}$

$$C_{\ell_p} = -m_{\ell\ell_B} \sin(\theta'_{\ell\ell_B} + \alpha) \tag{2.53}$$

The subscripts T and B refer again to the constants for the top and bottom surface, and these constants are generally different because of lack of symmetry of the upper and lower surface with respect to a C.G. outside the horizontal plane of symmetry. Of course these same equations will apply if the upper and lower part of the body are different in shape provided the constants are evaluated for each shape. In the case of the cone, the damping in roll constants happen to be an even function of the vertical and lateral position of the C.G., see Eqs. (2.42) and (2.43), and therefore the constants will be identical for the top and bottom.

For the slender cone, using the results of Eqs. (2.48) and (2.49), the damping in roll of the full cone assumes an especially simple analytic form throughout the angle of attack range.

$\alpha \leq -\frac{3\pi}{4}\theta$

$$C_{l_p} = -\frac{8}{3}\left(\frac{3_o}{c}\right)^2 \sin\left(\frac{3\pi}{4}\theta - \alpha\right) \tag{2.54}$$

$-\frac{3\pi}{4}\theta \leq \alpha \leq \frac{3\pi}{4}\theta$

$$C_{l_p} = -\frac{8}{3}\left(\frac{3_o}{c}\right)^2 \left[\sin\left(\frac{3\pi}{4}\theta + \alpha\right) + \sin\left(\frac{3\pi}{4}\theta - \alpha\right)\right] \tag{2.55}$$

$\alpha \geq \frac{3\pi}{4}\theta$

$$C_{l_p} = -\frac{8}{3}\left(\frac{3_o}{c}\right)^2 \sin\left(\frac{3\pi}{4}\theta + \alpha\right) \tag{2.56}$$

The damping in roll for a slender cone at zero angle of attack, with no lateral C.G. displacement, can be obtained from Eq. (2.55)

$$C_{l_p} = -4\pi\left(\frac{3_o}{c}\right)^2 \tag{2.57}$$

2.5 Damping in Yaw due to Rolling - C_{n_p}

The general analytic form of the damping in yaw due to rolling is presented in Section 5.5F and repeated here for convenience.

$$C_{n_p} = (k_{n_p})_1 \cos\alpha + (k_{n_p})_2 \sin\alpha \tag{5.54F}$$

$$C_{n_p} = m_{n_p} \sin(\theta_{n_p} + \alpha) \tag{5.55F}$$

where

$$m_{n_p} = \sqrt{(K_{n_p})_1^2 + (K_{n_p})_2^2} \tag{5.56F}$$

$$\theta_{n_p} = \tan^{-1} \frac{(K_{n_p})_1}{(K_{n_p})_2} = \sin^{-1} \frac{(K_{n_p})_1}{\sqrt{(K_{n_p})_1^2 + (K_{n_p})_2^2}} \tag{5.57F}$$

The constants have been determined for a half cone with flat side up at positive angles of attack as explained in Section 5.5F. The results are

$$(K_{n_p})_1 = -\frac{4\pi}{3}\left(\frac{z_o}{c}\right)\left[1 - \frac{3}{2}\left(\frac{x_o}{c}\right)\right]\tan\theta + 8\left(\frac{y_o}{c}\right)^2 \sin^2\theta - 2\pi\left(\frac{x_o}{c}\right)\left(\frac{z_o}{c}\right)\tan\theta \sin^2\theta \tag{2.58}$$

$$(K_{n_p})_2 = -\frac{16}{9}\left(\frac{z_o}{c}\right)\left[1 - \frac{3}{2}\left(\frac{x_o}{c}\right)\right] + 2\pi\left(\frac{y_o}{c}\right)^2 \tan\theta - \frac{8}{3}\left(\frac{x_o}{c}\right)\left(\frac{z_o}{c}\right)\sin^2\theta - 2\pi\left(\frac{y_o}{c}\right)^2 \tan\theta \sin^2\theta \tag{2.59}$$

For any cone angle (θ) and C.G. location (x_o, y_o, z_o), the constants can be evaluated numerically. The C_{n_p} as a function of angle of attack will then be defined by Eq. (5.54F) or (5.55F).

For a slender cone, assuming $y_o/c = 0$, and retaining only up to first order terms in the cone angle, considerable simplification is possible.

$$(K_{np})_1 = -\frac{4\pi}{3}\left(\frac{z_o}{c}\right)\left[1 - \frac{3}{2}\left(\frac{x_o}{c}\right)\right]\theta \tag{2.60}$$

$$(K_{np})_2 = -\frac{16}{9}\left(\frac{z_o}{c}\right)\left[1 - \frac{3}{2}\left(\frac{x_o}{c}\right)\right] \tag{2.61}$$

$$m_{np} = \frac{16}{9}\left(\frac{z_o}{c}\right)\left[1 - \frac{3}{2}\left(\frac{x_o}{c}\right)\right] \tag{2.62}$$

$$\theta_{np} = \pi + \theta'_{np} \qquad \text{where} \quad \theta'_{np} = \frac{3\pi}{4}\theta \tag{2.63}$$

Thus for slender half cone at positive angle of attack, Eq. (5.55F) becomes

$$C_{n_p} = -\frac{16}{9}\left(\frac{z_o}{c}\right)\left[1 - \frac{3}{2}\left(\frac{x_o}{c}\right)\right]\sin\left(\frac{3\pi}{4}\theta + \alpha\right) \tag{2.64}$$

The constants for C_{n_p} have been computed as a function of cone angle (θ), for fixed longitudinal C.G. locations (x_o/c), and zero lateral C.G. displacements ($y_o/c = 0$). The constants m_{np} and θ_{np} are plotted as Figs. 10, 11, and 12. The results show that C_{n_p} is a linear function of vertical C.G. position, and varies widely with longitudinal C.G. position. The damping is a minimum for the longitudinal C.G. located 2/3 of the cone length from the nose, and it will even change sign depending on the C.G. location. The results also demonstrate that Eq. (2.64) will give good results for half cone angles less than about 10 degrees.

The C_{n_p} of the complete cone can be found once the constants $(K_{np})_1$ and $(K_{np})_2$ of the upper half are determined. These were evaluated following the procedure in Section 5.5F. It was established that the $(K_{np})_1$ of the top can be obtained from $(K_{np})_1$ of the bottom by first substituting $-z_o$ for z_o,

and then changing the sign of all the terms. The $(K_{np})_2$ of the top is obtained from the bottom value by simply substituting $-z_o$ for z_o. The procedure to be followed in obtaining the C_{n_p} throughout the angle of attack range is similar to that used for the other derivatives.

2.6 Damping in Roll Due to Yawing - C_{ℓ_r}

The damping in roll due to yawing (C_{ℓ_r}) for the cone is the same as the C_{n_p} since the constants are identical.

$$(K_{np})_1 = (K_{\ell r})_1$$

$$(K_{np})_2 = (K_{\ell r})_2$$

It is also true that $(K_{\ell r})_1$ and $(K_{\ell r})_2$ for the top half of the cone bear the same relationships to the constants for the bottom half as that shown for $(K_{np})_1$ and $(K_{np})_2$. The alternate form of the C_{ℓ_r} constants, $(m_{\ell r})$ and $(\theta'_{\ell r})$, are also presented in Figs. 10, 11, and 12.

3.0 Analytic Equations - Delta Planform with Diamond Shape Cross-Section

3.1 General Discussion

Another aerodynamic shape that has been studied in some detail is the delta planform with diamond shaped cross-section in planes perpendicular to the longitudinal axis. All the surfaces of such a shape are flat planes. The important stability derivatives, both static and dynamic, have been determined for this shape. In the next quarter, the shape will be studied in some detail with controls added for purposes of trim at angle of attack. Stability derivatives will then be determined under trim condition, a primary goal in this whole study.

Results are presented for only a half body with the flat side up at positive angles of attack so that only the bottom surfaces "see" the flow. No discussion of analytic results are included here for the complete surface, top and bottom, at all angles of attack as was done for the cone. The procedure to be followed to obtain the derivatives of the whole body is essentially that discussed for the cone, and the cone results may be referred to for these details.

In the derivation of all the stability derivatives, the partial derivatives of the equation or equations of the surface are required. The body orientation and general shape, as well as the surface equations, will be shown here for convenient reference.

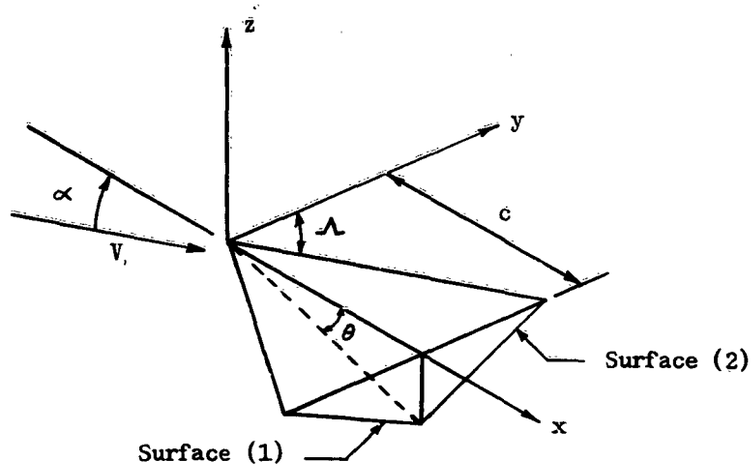

Surface (1)

$$F(x,y,z) = x + (\tan\Lambda)y + (\cot\theta)z = 0 \qquad (3.1)$$

Surface (2)

$$F(x,y,z) = x - (\tan\Lambda)y + (\cot\theta)z = 0 \qquad (3.2)$$

3.2 Longitudinal Force and Moment Equations

The forms of the longitudinal force and moment coefficient equations as derived in Section 3.0F are repeated below. The analytic equation for each coefficient can be written in either of the two basic forms.

$$C_A = (K_A)_1 \cos^2\alpha + (K_A)_2 \sin^2\alpha + (K_A)_3 \sin\alpha\cos\alpha \qquad (3.18F)$$

$$C_A = a_0 + a_1 \sin^2(\theta_a + \alpha) \qquad (3.19F)$$

$$C_N = (K_N)_1 \cos^2\alpha + (K_N)_2 \sin^2\alpha + (K_N)_3 \sin\alpha\cos\alpha \qquad (3.31F)$$

$$C_N = n_0 + n_1 \sin^2(\theta_n + \alpha) \qquad (3.35F)$$

$$C_m = (K_m)_1 \cos^2\alpha + (K_m)_2 \sin^2\alpha + (K_m)_3 \sin\alpha\cos\alpha \qquad (3.40F)$$

$$C_m = m_0 + m_1 \sin^2(\theta_m + \alpha) \qquad (3.44F)$$

The integral relationships and equations for evaluating these constants are presented in Section 3.0F. These integral relationships are used in conjunction with the equations of the surface, Eqs. (3.1) and (3.2).

For the half body at positive angles of attack, the constants have been evaluated and are shown below.

$$(K_A)_1 = \frac{2\tan\theta\sin^2\theta}{1+\sin^2\theta\tan^2\Lambda} \qquad a_0 = 0$$

$$(K_A)_2 = \frac{2\sin\theta\cos\theta}{1+\sin^2\theta\tan^2\Lambda} \qquad a_1 = \frac{2\tan\theta}{1+\sin^2\theta\tan^2\Lambda}$$

$$(K_A)_3 = \frac{4\sin^2\theta}{1+\sin^2\theta\tan^2\Lambda} \qquad \theta_a = \theta$$

$$(K_N)_1 = \frac{2\sin^2\theta}{1+\sin^2\theta\tan^2\Lambda} \qquad n_0 = 0$$

$$(K_N)_2 = \frac{2\cos^2\theta}{1+\sin^2\theta\tan^2\Lambda} \qquad n_1 = \frac{2}{1+\sin^2\theta\tan^2\Lambda}$$

$$(K_N)_3 = \frac{4\sin\theta\cos\theta}{1+\sin^2\theta\tan^2\Lambda} \qquad \theta_n = \theta$$

$$(K_m)_1 = \frac{-\frac{2}{3}\tan^2\theta\sin^2\theta}{1+\sin^2\theta\tan^2\Lambda} \qquad m_0 = 0$$

$$(K_m)_2 = \frac{-\frac{2}{3}\sin^2\theta}{1+\sin^2\theta\tan^2\Lambda} \qquad m_1 = \frac{\frac{2}{3}\tan^2\theta}{1+\sin^2\theta\tan^2\Lambda}$$

$$(K_m)_3 = \frac{-\frac{4}{3}\tan\theta\sin^2\theta}{1+\sin^2\theta\tan^2\Lambda} \qquad \theta_m = \frac{\pi}{2} + \theta_m' \text{ , where } \theta_m' = \theta$$

The more useful form of the analytic expressions for the longitudinal force and moment coefficients are expressed by Eqs. (3.19F), (3.35F), and (3.44F). In ter ⌟ of the evaluated coefficients these equations become,

$$C_A = \frac{2\tan\theta}{1+\sin^2\theta\tan^2\Lambda}\sin^2(\theta+\alpha) \tag{3.3}$$

$$C_N = \frac{2}{1+\sin^2\theta\tan^2\Lambda}\sin^2(\theta+\alpha) \tag{3.4}$$

$$C_m = \frac{-\frac{2}{3}\tan^2\theta}{1+\sin^2\theta\tan^2\Lambda}\sin^2(\theta+\alpha) \tag{3.5}$$

Eq. (3.5) is evaluated for a C. G. located 2/3 of the body length aft of the nose on the longitudinal x axis.

It is interesting to note that in all cases the "effective" body angles (θ_a, θ_n, θ'_m) are equal to the geometric angle θ. When these expressions are used in determining the forces and moments of the full body throughout the angle of attack range, the resulting equations are exact since complete masking or unmasking of the bottom and top occurs precisely at angles of attack - θ and + θ respectively. The complete surface results can be obtained in a manner identical to that shown for the full cone in Section 6.1F.

3.3 Lateral Directional Static Stability Derivatives

The static lateral-directional stability derivatives for a surface can be defined analytically in the following forms as demonstrated in Section 4.3F.

$$C_{Y_\beta} = (K_{Y\beta})_1 \cos\alpha + (K_{Y\beta})_2 \sin\alpha \qquad (4.28F)$$

$$C_{Y_\beta} = Y_\beta \sin(\theta_{Y\beta} + \alpha) \qquad (4.32F)$$

$$C_{l_\beta} = (K_{l\beta})_1 \cos\alpha + (K_{l\beta})_2 \sin\alpha \qquad (4.35F)$$

$$C_{l_\beta} = l_\beta \sin(\theta_{l\beta} + \alpha) \qquad (4.38F)$$

$$C_{n_\beta} = (K_{n\beta})_1 \cos\alpha + (K_{n\beta})_2 \sin\alpha \qquad (4.43F)$$

$$C_{n_\beta} = n_\beta \sin(\theta_{n\beta} + \alpha) \qquad (4.46F)$$

The integral relationships and equations for evaluating these constants are shown in Section 4.3F. The equations of the surface that must be used are Eqs. (3.1) and (3.2). For the half body, the following values of the constants were obtained.

$$(K_{\gamma\beta})_1 = \frac{-4\tan\theta\sin^2\theta\tan^2\Lambda}{1+\sin^2\theta\tan^2\Lambda} \qquad Y_\beta = \frac{4\tan\theta\sin\theta\tan^2\Lambda}{1+\sin^2\theta\tan^2\Lambda}$$

$$(K_{\gamma\beta})_2 = \frac{-4\sin^2\theta\tan^2\Lambda}{1+\sin^2\theta\tan^2\Lambda} \qquad \theta_{\gamma\beta} = \pi + \theta'_{\gamma\beta}\ , \quad \text{where} \quad \theta'_{\gamma\beta} = \theta$$

$$(K_{\ell\beta})_1 = \frac{-\frac{4}{3}\sin^2\theta\left\{1-\tan\theta\tan^2\Lambda\left[\tan\theta+3\left(\frac{\delta_\ell}{c}\right)\right]\right\}}{1+\sin^2\theta\tan^2\Lambda}$$

$$(K_{\ell\beta})_2 = \frac{-\frac{4}{3}\sin\theta\cos\theta\left\{1-\tan\theta\tan^2\Lambda\left[\tan\theta+3\left(\frac{\delta_\ell}{c}\right)\right]\right\}}{1+\sin^2\theta\tan^2\Lambda}$$

$$\ell_\beta = \frac{\frac{4}{3}\sin\theta\left\{1-\tan\theta\tan^2\Lambda\left[\tan\theta+3\left(\frac{\delta_\ell}{c}\right)\right]\right\}}{1+\sin^2\theta\tan^2\Lambda}$$

$$\theta_{\ell\beta} = \pi + \theta'_{\ell\beta}\ , \qquad \text{where} \quad \theta'_{\ell\beta} = \theta$$

$$(K_{n\beta})_1 = \frac{\frac{4}{3}\tan\theta\sin^2\theta\left\{1+2\tan^2\Lambda\left[1-\frac{3}{2}\left(\frac{\chi_\theta}{c}\right)\right]\right\}}{1+\sin^2\theta\tan^2\Lambda}$$

$$(K_{n\beta})_2 = \frac{\frac{4}{3}\sin^2\theta\left\{1+2\tan^2\Lambda\left[1-\frac{3}{2}\left(\frac{\chi_\theta}{c}\right)\right]\right\}}{1+\sin^2\theta\tan^2\Lambda}$$

$$n_\beta = \frac{\frac{4}{3}\tan\theta\sin\theta\left\{1+2\tan^2\Lambda\left[1-\frac{3}{2}\left(\frac{x_o}{c}\right)\right]\right\}}{1+\sin^2\theta\tan^2\Lambda}$$

$$\theta_{n\beta} = \theta'_{n\beta} = \theta$$

The more useful form of the lateral-directional static stability derivatives are those expressed by Eqs. (4.32F), (4.38F), and (4.46F). For the moment center located at $(z_o/c) = 0$ and $(x_o/c) = 2/3$, these equations become especially simple in terms of the evaluated constants.

$$C_{Y_\beta} = \frac{-4\tan\theta\sin\theta\tan^2\Lambda}{1+\sin^2\theta\tan^2\Lambda}\sin(\theta+\alpha) \tag{3.6}$$

$$C_{l_\beta} = \frac{-\frac{4}{3}\sin\theta(1-\tan^2\theta\tan^2\Lambda)}{1+\sin^2\theta\tan^2\Lambda}\sin(\theta+\alpha) \tag{3.7}$$

$$C_{n_\beta} = \frac{\frac{4}{3}\tan\theta\sin\theta}{1+\sin^2\theta\tan^2\Lambda}\sin(\theta+\alpha) \tag{3.8}$$

The effective body angles $\theta'_{Y\beta}$, $\theta'_{l\beta}$, and $\theta'_{n\beta}$ are again equal to the geometric angle θ. The lateral-directional static stability derivatives for the complete surface can be obtained in the manner indicated for the full cone in Section 6.2F.

3.4 Damping in Pitch - C_{m_q}

The derivation of the damping in pitch equations are shown in Section 5.2F. The damping in pitch can be expressed in one of two ways.

$$C_{m_q} = (K_{m_q})_1\cos\alpha + (K_{m_q})_2\sin\alpha \tag{5.17F}$$

$$C_{m_q} = m_q \sin(\theta_{m_q} + \alpha) \qquad (5.18F)$$

The method for evaluating the constants in these equations is also shown in Section 5.2F.

For the half diamond shape body at positive angles of attack, the constants assume the following form:

$$(K_{mq})_1 = \frac{-4\left[1 - \frac{8}{3}\left(\frac{x_0}{c}\right) + 2\left(\frac{x_0}{c}\right)^2\right]\tan\theta}{1 + \sin^2\theta \tan^2\Lambda} - \frac{\frac{32}{3}\left(\frac{d_0}{c}\right)\left[1 - \frac{3}{4}\left(\frac{x_0}{c}\right)\right]\sin^2\theta}{1 + \sin^2\theta \tan^2\Lambda} -$$

$$- \frac{8\left[\left(\frac{d_0}{c}\right)^2 + \frac{2}{3}\left(\frac{x_0}{c}\right) - \left(\frac{x_0}{c}\right)^2\right]\tan\theta \sin^2\theta}{1 + \sin^2\theta \tan^2\Lambda} -$$

$$- \frac{\frac{16}{3}\left(\frac{d_0}{c}\right)\tan^2\theta \sin^2\theta}{1 + \sin^2\theta \tan^2\Lambda} - \frac{\frac{4}{3}\tan^3\theta \sin^2\theta}{1 + \sin^2\theta \tan^2\Lambda}$$

$$(K_{mq})_2 = \frac{-4\left[1 - \frac{8}{3}\left(\frac{x_0}{c}\right) + 2\left(\frac{x_0}{c}\right)^2\right]}{1 + \sin^2\theta \tan^2\Lambda} - \frac{\frac{32}{3}\left(\frac{d_0}{c}\right)\left[1 - \frac{3}{4}\left(\frac{x_0}{c}\right)\right]\tan\theta}{1 + \sin^2\theta \tan^2\Lambda} -$$

$$- \frac{8\left[\left(\frac{d_0}{c}\right)^2 + \frac{2}{3}\left(\frac{x_0}{c}\right) - \left(\frac{x_0}{c}\right)^2\right]\sin^2\theta}{1 + \sin^2\theta \tan^2\Lambda} +$$

$$+ \frac{\frac{16}{3}\left(\frac{d_0}{c}\right)\left[1 - 3\left(\frac{x_0}{c}\right)\right]\tan\theta \sin^2\theta}{1 + \sin^2\theta \tan^2\Lambda} - \frac{\frac{4}{3}\tan^2\theta \sin^2\theta}{1 + \sin^2\theta \tan^2\Lambda}$$

$$m_q = \frac{4\sec\theta}{1+\sin^2\theta\tan^2\Lambda}\left\{\left[1-\frac{8}{3}\left(\frac{x_o}{c}\right)+2\left(\frac{x_o}{c}\right)^2\right]+\frac{8}{3}\left(\frac{z_o}{c}\right)\left[1-\frac{3}{2}\left(\frac{x_o}{c}\right)\right]\tan\theta+\right.$$

$$+2\left[\left(\frac{z_o}{c}\right)^2+\frac{2}{3}\left(\frac{x_o}{c}\right)-\left(\frac{x_o}{c}\right)^2\right]\sin^2\theta-\frac{4}{3}\left(\frac{z_o}{c}\right)\left[1-3\left(\frac{x_o}{c}\right)\right]\tan\theta\sin^2\theta+$$

$$\left.+\frac{1}{3}\tan^2\theta\sin^2\theta\right\}$$

$$\theta_{mq} = \pi + \theta'_{mq}\ , \qquad \text{where} \quad \theta'_{mq} = \theta$$

The pitch damping constants are rather involved functions of the longitudinal and vertical C. G. location. These constants can of course be evaluated numerically for any C. G. location and values of the angles θ and Λ. In the case of small θ's, if tan Λ is of the order of one or less, and the vertical C. G. is located within the body ($\left|\frac{z_o}{x_o}\right| < \tan\theta$), considerable simplification is possible. Retaining only up to first order terms in θ and z_o/c, Eq. (5.18F) becomes

$$C_{m_q} = -4\left[1-\frac{8}{3}\left(\frac{x_o}{c}\right)+2\left(\frac{x_o}{c}\right)^2\right]\sin(\theta+\alpha) \qquad (3.9)$$

Equation (3.9) should be compared to Eq. (2.7) for the half cone. In the limit, as θ approaches zero, Eq. (3.9) becomes the damping of a flat plate delta surface at angle of attack.

3.5 Lateral-Directional Damping Derivatives - C_{n_r}, C_{ℓ_p}, C_{n_p}, C_{ℓ_r}

The form of the lateral-directional damping derivatives are determined in Sections 5.3F, 5.4F, 5.5F, and 5.6F. The integral relationships and equations for evaluating the constants in the damping derivative equations are also presented in these sections. For convenience, the two forms of each damping derivative equation are shown again below.

$$C_{n_r} = (K_{nr})_1 \cos\alpha + (K_{nr})_2 \sin\alpha \qquad (5.28F)$$

$$C_{n_r} = m_{nr} \sin(\theta_{nr} + \alpha) \qquad (5.31F)$$

$$C_{\ell_p} = (K_{\ell p})_1 \cos\alpha + (K_{\ell p})_2 \sin\alpha \qquad (5.43F)$$

$$C_{\ell_p} = m_{\ell p} \sin(\theta_{\ell p} + \alpha) \qquad (5.44F)$$

$$C_{n_p} = (K_{np})_1 \cos\alpha + (K_{np})_2 \sin\alpha \qquad (5.54F)$$

$$C_{n_p} = m_{np} \sin(\theta_{np} + \alpha) \qquad (5.55F)$$

$$C_{\ell_r} = (K_{\ell r})_1 \cos\alpha + (K_{\ell r})_2 \sin\alpha \qquad (5.64F)$$

$$C_{\ell_r} = m_{\ell r} \sin(\theta_{\ell r} + \alpha) \qquad (5.65F)$$

The constants in these equations for the half body at positive angles of attack have been evaluated. It was discovered early in the integration process for determining the constants that some simplification was possible. For the shape under consideration, the following relations hold:

$(K_{nr})_1 = \tan\theta (K_{nr})_2$ $\qquad$ $m_{nr} = -\sec\theta (K_{nr})_2$ $\qquad$ $\theta_{nr} = \pi + \theta'_{nr}$, where $\theta'_{nr} = \theta$

$(K_{\ell p})_1 = \tan\theta (K_{\ell p})_2$ $\qquad$ $m_{\ell p} = -\sec\theta (K_{\ell p})_2$ $\qquad$ $\theta_{\ell p} = \pi + \theta'_{\ell p}$, where $\theta'_{\ell p} = \theta$

$(K_{np})_1 = \tan\theta (K_{np})_2$ $\qquad$ $m_{np} = \sec\theta (K_{np})_2$ $\qquad$ $\theta_{np} = \theta'_{np} = \theta$

$(K_{\ell r})_1 = \tan\theta (K_{\ell r})_2$ $\qquad$ $m_{\ell r} = \sec\theta (K_{\ell r})_2$ $\qquad$ $\theta_{\ell r} = \theta'_{\ell r} = \theta$

An examination of the damping in pitch, and the lateral-directional static stability derivatives discussed in Sections 3.4 and 3.3 shows that similar relationships hold for these derivatives. Listed below are only the values of $(K_{nr})_2$, $(K_{lp})_2$, $(K_{np})_2$, and $(K_{lr})_2$, since from these the other constants can be easily determined.

$$(K_{nr})_2 = \frac{-4\sin^2\theta\left\{\left[1-\frac{4}{3}\left(\frac{x_o}{c}\right)+2\left(\frac{y_o}{c}\right)^2\right]+\left[1-\frac{8}{3}\left(\frac{x_o}{c}\right)+2\left(\frac{x_o}{c}\right)^2\right]\tan^2\Lambda+\frac{1}{3}\cot^2\Lambda\right\}}{1+\sin^2\theta\tan^2\Lambda}$$

$$(K_{lp})_2 = \frac{-\frac{4}{3}}{1+\sin^2\theta\tan^2\Lambda}\left\{\left[\cot^2\Lambda+6\left(\frac{y_o}{c}\right)^2\right]-4\left(\frac{z_o}{c}\right)\tan\theta-\right.$$

$$-\left[1+6\left(\frac{z_o}{c}\right)^2\tan\Lambda+\cot^2\Lambda+6\left(\frac{y_o}{c}\right)^2\right]\sin^2\theta+$$

$$\left.+4\left(\frac{z_o}{c}\right)\left[1+\tan\Lambda\right]\tan\theta\sin^2\theta+\tan\Lambda\tan^2\theta\sin^2\theta\right\}$$

$$(K_{np})_2=(K_{lr})_2=\frac{2}{1+\sin^2\theta\tan^2\Lambda}\left\{\left[1-\frac{4}{3}\left(\frac{x_o}{c}\right)+\frac{2}{3}\cot^2\Lambda+4\left(\frac{y_o}{c}\right)^2\right]\tan\theta-\right.$$

$$-\frac{4}{3}\left(\frac{z_o}{c}\right)\left[1-2\left(1+\frac{3}{2}\frac{x_o}{c}\right)\tan^2\Lambda\right]\sin^2\theta-$$

$$\left.-\frac{4}{3}\left[1+3\left(\frac{y_o}{c}\right)^2-\left(\frac{x_o}{c}\right)\left(1-\tan^2\Lambda\right)+\frac{3}{4}\tan^2\Lambda+\frac{1}{4}\cot^2\Lambda\right]\tan\theta\sin^2\theta\right\}$$

It is of interest to note that the cross-damping derivatives, C_{np} and C_{lr}, will be identical since $(K_{np})_2$ and $(K_{lr})_2$ are equal.

Considerable simplification is possible in the equations for evaluating the constants if one assume that the C.G. lies on the x axis ($z_o/c = 0$, $y_o/c = 0$).

Under this assumption the constants become

$$(K_{nr})_2 = \frac{-4\sin^2\theta}{1+\sin^2\theta\tan^2\lambda}\left\{\left[1-\frac{4}{3}\left(\frac{\chi_0}{c}\right)\right]+\left[1-\frac{8}{3}\left(\frac{\chi_0}{c}\right)+2\left(\frac{\chi_0}{c}\right)^2\right]\tan^2\lambda+\frac{1}{3}\cot^2\lambda\right\}$$

$$(K_{\ell p})_2 = \frac{-\frac{4}{3}}{1+\sin^2\theta\tan^2\lambda}\left\{\cot^2\lambda-\left[1+\cot^2\lambda\right]\sin^2\theta+\tan\lambda\tan^2\theta\sin^2\theta\right\}$$

$$(K_{np})_2 = (K_{\ell r})_2 = \frac{2}{1+\sin^2\theta\tan^2\lambda}\left\{\left[1-\frac{4}{3}\left(\frac{\chi_0}{c}\right)+\frac{2}{3}\cot^2\lambda\right]\tan\theta-\right.$$

$$\left.-\frac{4}{3}\left[1-\left(\frac{\chi_0}{c}\right)\left(1-\tan^2\lambda\right)+\frac{3}{4}\tan^2\lambda+\frac{1}{2}\cot^2\lambda\right]\tan\theta\sin^2\theta\right\}$$

If the further assumption is made that θ is a small angle, and tan λ is of the order of 1 or less, then further simplification is possible in the constants. Retaining only the lowest order term in θ for each constant we have

$$(K_{nr})_2 = -4\left\{\left[1-\frac{4}{3}\left(\frac{\chi_0}{c}\right)\right]+\left[1-\frac{8}{3}\left(\frac{\chi_0}{c}\right)+2\left(\frac{\chi_0}{c}\right)^2\right]\tan^2\lambda+\frac{1}{3}\cot^2\lambda\right\}\theta^2$$

$$(K_{\ell p})_2 = -\frac{4}{3}\cot^2\lambda$$

$$(K_{np})_2 = (K_{\ell r})_2 = 2\left[1-\frac{4}{3}\left(\frac{\chi_0}{c}\right)+\frac{4}{3}\cot^2\lambda\right]\theta$$

With these assumptions, the constants m_{nr}, $m_{\ell p}$, m_{np}, and $m_{\ell r}$ are identical to $(K_{nr})_2$, $(K_{\ell p})_2$, $(K_{np})_2$, and $(K_{\ell r})_2$ respectively.

Now, for the half diamond shape body at positive angles of attack, the lateral-directional damping derivatives assume the following simplified form.

$$C_{n_r} = -4\left\{\left[1-\frac{4}{3}\left(\frac{x_o}{c}\right)\right]+\left[1-\frac{8}{3}\left(\frac{x_o}{c}\right)+2\left(\frac{x_o}{c}\right)^2\right]\tan^2\Lambda+\frac{1}{3}\cot^2\Lambda\right\}\theta^2\sin(\theta+\alpha) \qquad (3.10)$$

$$C_{l_p} = -\frac{4}{3}\cot^2\Lambda\sin(\theta+\alpha) \qquad (3.11)$$

$$C_{n_p} = C_{l_r} = 2\left[1-\frac{4}{3}\left(\frac{x_o}{c}\right)+\frac{2}{3}\cot^2\Lambda\right]\theta\sin(\theta+\alpha) \qquad (3.12)$$

In the limiting case of $\theta = 0$, Eqs. (3.10), (3.11), and (3.12) become the damping derivatives of a flat plate delta surface with sweepback Λ . For this case

$$C_{l_p} = -\frac{4}{3}\cot^2\Lambda\sin\alpha \qquad (3.13)$$

$$C_{n_r} = C_{n_p} = C_{l_r} = 0 \qquad (3.14)$$

It is possible to look at other limiting forms of the surface with diamond shape cross-section. If one assumes that $\cot\Lambda = \tan\theta$, then the shape is one that can be inscribed in a cone. One can then make interesting comparisons between the derivatives of this shape and those of a cone.

4.0 Analytic Equations - The Elliptic Cone

4.1 General Discussion

An aerodynamic shape of some interest upon which some initial investigations have been made is the elliptic cone. Only analytic equations for axial and normal force coefficients have been determined up to now and the results are presented here. The moments and the lateral-directional stability derivatives

will be determined in the next quarter.

The results for only a half body with flat side up at positive angles of attack are presented. The equations for the complete surface at all angles of attack can be easily obtained using the procedure discussed for the cone in Section 6.1F.

A sketch of the half elliptic cone body and the equation of the surface required in the analysis is shown below.

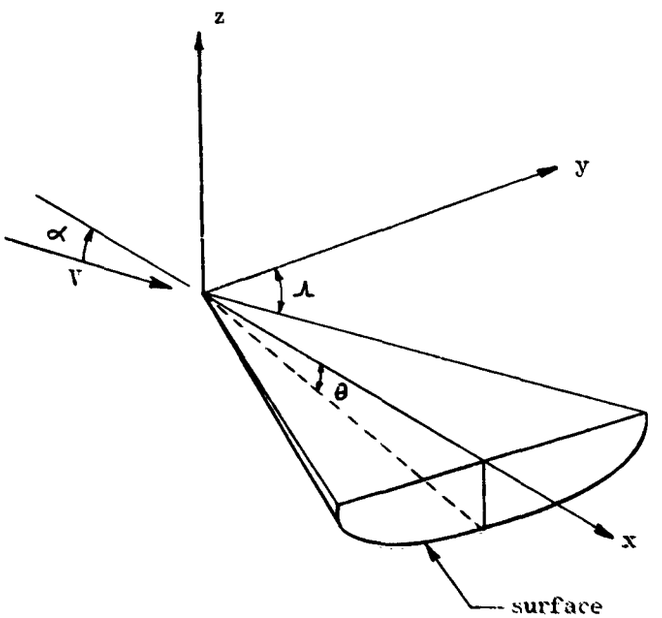

Equation of the surface:

$$F(x,y,z) = x^2 - (\tan^2\lambda)y^2 - (\cot^2\theta)z^2 = 0$$

4.2 Longitudinal Force Equations

The general form of the longitudinal force equations are derived

in Section 3.0F and presented in Section 3.2. The integral relationships and equations required to determine the constants in these equations are shown in Section 3.0F. For the half elliptic cone body the constants become

$$(K_A)_1 = \pi \cos\Lambda \tan\theta \sin\theta$$

$$(K_A)_2 = \frac{\pi \cos\Lambda \sin\theta \cos\theta}{\cos\Lambda + \sin\theta}$$

$$(K_A)_3 = \frac{2\sin^2\theta}{\left[1-\left(\frac{\sin\theta}{\cos\Lambda}\right)^2\right]^{1/2}} \log \left| \frac{1+\left[1-\left(\frac{\sin\theta}{\cos\Lambda}\right)^2\right]^{1/2}}{1-\left[1-\left(\frac{\sin\theta}{\cos\Lambda}\right)^2\right]^{1/2}} \right| \qquad \frac{\sin\theta}{\cos\Lambda} < 1$$

$$(K_A)_3 = \frac{-4\sin^2\theta}{\left[\left(\frac{\sin\theta}{\cos\Lambda}\right)^2 - 1\right]^{1/2}} \left\{ \cot^{-1}\left[\left(\frac{\sin\theta}{\cos\Lambda}\right)^2 - 1\right]^{1/2} - \frac{\pi}{2} \right\} \qquad \frac{\sin\theta}{\cos\Lambda} > 1$$

$$(K_N)_1 = \frac{2\sin\theta}{\tan\Lambda\left[1-\left(\frac{\cot\Lambda}{\tan\theta}\right)^2\right]^{1/2}} \tan^{-1}\left\{ \sin\theta \tan\Lambda \left[1-\left(\frac{\cot\Lambda}{\tan\theta}\right)^2\right]^{1/2} \right\} \qquad \frac{\cot\Lambda}{\tan\theta} < 1$$

$$(K_N)_1 = \frac{\sin\theta}{\tan\Lambda\left[\left(\frac{\cot\Lambda}{\tan\theta}\right)^2 - 1\right]^{1/2}} \log \left| \frac{1+\sin\theta\tan\Lambda\left[\left(\frac{\cot\Lambda}{\tan\theta}\right)^2-1\right]^{1/2}}{1-\sin\theta\tan\Lambda\left[\left(\frac{\cot\Lambda}{\tan\theta}\right)^2-1\right]^{1/2}} \right| \qquad \frac{\cot\Lambda}{\tan\theta} > 1$$

$$(K_N)_2 = \frac{-2\cos^2\theta}{\sin^2\theta(\tan^2\Lambda - \cot^2\theta)}\left[1 - \frac{\sin^2\theta\sec^2\Lambda}{\sin\theta\sqrt{\tan^2\Lambda - \cot^2\theta}}\tan^{-1}\left(\sin\theta\sqrt{\tan^2\Lambda - \cot^2\theta}\right)\right]$$

$$\frac{\cot\Lambda}{\tan\theta} < 1$$

$$(K_N)_2 = \frac{2\cos^2\theta}{\sin^2\theta(\cot^2\theta - \tan^2\Lambda)}\left[1 - \frac{\sin^2\theta\sec^2\Lambda}{2\sin\theta\sqrt{\cot^2\theta - \tan^2\Lambda}}\log\left|\frac{1+\sin\theta\sqrt{\cot^2\theta - \tan^2\Lambda}}{1-\sin\theta\sqrt{\cot^2\theta - \tan^2\Lambda}}\right|\right]$$

$$\frac{\cot\Lambda}{\tan\theta} > 1$$

$$(K_N)_3 = \frac{2\pi\cos\theta}{\csc\theta + \sec\Lambda}$$

For any values of the angles Λ and θ, numerical evaluation of the constants in Eqs. (3.18F), (3.19F), (3.31F), and (3.35F) become obvious following the procedure outlined in Section 3.0F.

It should be of interest to examine slender elliptic cones of various fixed ratios of the two axes of the ellipse. From the previous sketch, the ratio of horizontal to vertical axes of the ellipse (e) is obviously

$$e = \frac{\cot\Lambda}{\tan\theta}$$

If the assumption is now made that the angle θ is small, and e is of the order of one, it is possible to obtain quite simple analytic expressions for the constants in terms of e and the angle θ. If the value of e is fixed, then the constants become only a function of θ. For small θ's, the constants are listed below for three ellipses.

	e = 2.0	e = 1.0	e = 1/2
a_o	$1.8642\theta^3$	$.5951\theta^3$	$.4756\theta^3$
a_1	2.0944θ	1.5708θ	1.0472θ
θ_a	1.452θ	1.2732θ	1.1547θ
n_o	$.3944\theta^2$	$.1488\theta^2$	$.04925\theta^2$
n_1	1.6528	1.3333	.9455
θ_n	1.2671θ	1.1784θ	1.1075θ

The constants for e = 1.0 (the circular cone) are taken from Section 6.1F. These results will be studied in more detail to determine the range of θ's over which they are reasonably valid. The pitching moments and some of the damping derivatives for the elliptic cone will also be evaluated.

5.0 Analytic Equations for the Stability Derivatives Considering Bluntness

5.1 Introduction

All the body shapes that have been analyzed up to this point have had surfaces whose shape can be expressed by a single equation. It has also been stated elsewhere in this report that the methods are still applicable if the top and bottom of the body can each be expressed by different equations, since the top and bottom of the body are analyzed separately. These general relationships also hold for bodies whose surfaces are composites of two or more shapes, such as a spherical cap and a cone. The only details to be studied are how the results for the different shapes are to be combined to obtain the aerodynamic characteristics of the complete body.

Surfaces of special interest at hypersonic speeds are those with blunted noses and leading edges. Some preliminary investigations have been made of the application of the general methods shown in the "First Quarterly Technical Report" to a blunted cone, and these results are presented in this section.

5.2 Analytic Equations - The Spherical Cap

In order to analyze the aerodynamic characteristics and stability derivatives of a spherically blunted cone, it is necessary first to determine the properties of the spherical cap. Analytic equations for the force and moment coefficients, and the stability derivatives of a spherical cap can be determined in the same manner as that used for the cone or any other surface. The basic methods are presented in Sections 3.0F, 4.0F, and 5.0F. The basic equations will not be repeated, only the values of the constants in these equations are tabulated below for the bottom half of a cap at positive angles of attack.

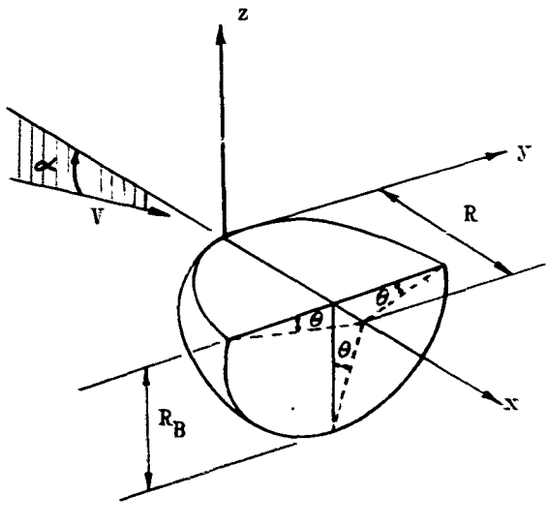

Equation of the Spherical Cap Segment

$$-(x-R)^2-y^2-z^2+R^2=0$$

Longitudinal Force and Moment Coefficient Constants for C_A, C_N, and C_m

$$(K_A)_1 = 1+\sin^2\theta$$

$$(K_A)_2 = \tfrac{1}{2}\cos^2\theta$$

$$(K_A)_3 = \frac{(1-\frac{2}{\pi}\theta)}{\cos^2\theta}\left[1+\frac{\sin 4\theta}{2\pi(1-\frac{2}{\pi}\theta)}\right]$$

$$(K_N)_1 = \frac{\frac{1}{2}(1-\frac{2}{\pi}\theta)}{\cos^2\theta}\left[1+\frac{\sin 4\theta}{2\pi(1-\frac{2}{\pi}\theta)}\right]$$

$$(K_N)_2 = \frac{(1-\frac{2}{\pi}\theta)}{\cos^2\theta}\left[1-\frac{4\sin 2\theta}{3\pi(1-\frac{2}{\pi}\theta)}-\frac{\sin 4\theta}{6\pi(1-\frac{2}{\pi}\theta)}\right]$$

$$(K_N)_3 = \cos^2\theta$$

$$(K_m)_1 = (K_m)_2 = (K_m)_3 = 0$$

Lateral-Directional Static Stability Constants for C_{Y_β}, C_{n_β} and C_{l_β}

$$(K_{Y\beta})_1 = -\cos^2\theta$$

$$(K_{Y3})_2 = \frac{-(1-\frac{2}{\pi}\theta)}{\cos^2\theta}\left[1-\frac{4\sin 2\theta}{3\pi(1-\frac{2}{\pi}\theta)}-\frac{\sin 4\theta}{6\pi(1-\frac{2}{\pi}\theta)}\right]$$

$$(K_{l\beta})_1 = (K_{l\beta})_2 = (K_{n\beta})_1 = (K_{n\beta})_2 = 0$$

Longitudinal Damping Constants for C_{m_q}

$$(K_{mq})_1 = -2\left[\left(1-\frac{x_0}{R}\right)^2 + 2\left(1-\frac{x_0}{R}\right)\left(\frac{z_0}{R}\right) + 2\left(\frac{z_0}{R}\right)^2\right] + \frac{8}{\pi}\left(1-\frac{x_0}{R}\right)\left(\frac{z_0}{R}\right)(\theta - \tan\theta) -$$

$$- 8\left(\frac{z_0}{R}\right)\left[\left(1-\frac{x_0}{R}\right) + \left(\frac{z_0}{R}\right)\right]\tan^2\theta + \frac{8}{3\pi}\left(1-\frac{x_0}{R}\right)\left(\frac{z_0}{R}\right)(2\theta + \tan\theta)\tan^2\theta -$$

$$- 4\left(1-\frac{x_0}{R}\right)\left(\frac{z_0}{R}\right)\tan^4\theta + \frac{8}{3\pi}\left(1-\frac{x_0}{R}\right)\left(\frac{z_0}{R}\right)\theta\tan^4\theta$$

$$(K_{mq})_2 = -4\left(1-\frac{x_0}{R}\right)\left(\frac{z_0}{R}\right) - 2\left[2\left(1-\frac{x_0}{R}\right)^2 + \left(\frac{z_0}{R}\right)^2\right]\left\{1 - \frac{2}{\pi}\theta - \right.$$

$$- \frac{\left[\frac{10}{3}\left(1-\frac{x_0}{R}\right)^2 - \left(\frac{z_0}{R}\right)^2\right]}{\left[2\left(1-\frac{x_0}{R}\right)^2 + \left(\frac{z_0}{R}\right)^2\right]}\frac{2}{\pi}\tan\theta + 2\tan^2\theta - \frac{4}{3\pi}\theta\tan^2\theta -$$

$$\left. - \frac{2}{\pi}\tan^3\theta + \tan^4\theta - \frac{2}{\pi}\theta\tan^4\theta\right\}$$

Lateral-Directional Damping Constants for C_{n_r}, C_{ℓ_p}, C_{n_p}, and C_{ℓ_r}

$$(K_{nr})_1 = -2\left(1-\frac{x_0}{R}\right)^2 - 4\left(\frac{y_0}{R}\right)^2 - 8\left(\frac{y_0}{R}\right)^2\tan^2\theta$$

$$(K_{nr})_2 = -2\left[\left(1-\frac{x_0}{R}\right)^2 + \frac{1}{8}\left(\frac{y_0}{R}\right)^2\right]\left\{1 - \frac{2}{\pi}\theta - \frac{\left[\left(1-\frac{x_0}{R}\right)^2 - \frac{3}{10}\left(\frac{y_0}{R}\right)^2\right]}{\left[\left(1-\frac{x_0}{R}\right)^2 + \frac{1}{8}\left(\frac{y_0}{R}\right)^2\right]}\frac{10}{3\pi}\tan\theta + \right.$$

$$\left. + 2\tan^2\theta - \frac{4}{3\pi}\theta\tan^2\theta - \frac{2}{\pi}\tan^3\theta + \tan^4\theta - \frac{2}{\pi}\theta\tan^4\theta\right\}$$

$$(K_{\ell p})_1 = -2\left[\left(\frac{y_0}{R}\right)^2 + \left(\frac{z_0}{R}\right)^2\right]$$

$$(K_{\ell p})_2 = -2\left[2\left(\frac{y_0}{R}\right)^2 + \left(\frac{z_0}{R}\right)^2\right]\left\{1 - \frac{2}{\pi}\theta - \frac{10}{3\pi}\tan\theta + 2\tan^2\theta - \right.$$

$$\left. - \frac{4}{\pi}\theta\tan^2\theta - \frac{2}{\pi}\tan^3\theta + \tan^4\theta - \frac{2}{\pi}\theta\tan^4\theta\right\}$$

$$(K_{np})_1 = (K_{\ell r})_1 = -2\left(1 - \frac{x_0}{R}\right)\left(\frac{z_0}{R}\right) + 2\left(\frac{y_0}{R}\right)^2\left\{1 - \frac{2}{\pi}\theta + \frac{2}{\pi}\tan\theta + \right.$$

$$+ 2\tan^2\theta - \frac{4}{\pi}\theta\tan^2\theta - \frac{2}{\pi}\tan^3\theta + \tan^4\theta -$$

$$\left. - \frac{2}{\pi}\theta\tan^4\theta\right\}$$

$$(K_{np})_2 = (K_{\ell r})_2 = 2\left(\frac{y_0}{R}\right)^2 - 2\left(1 - \frac{x_0}{R}\right)\left(\frac{z_0}{R}\right)\left\{1 - \frac{2}{\pi}\theta - \frac{10}{3\pi}\tan\theta + \right.$$

$$+ 2\tan^2\theta - \frac{4}{\pi}\theta\tan^2\theta - \frac{2}{\pi}\tan^3\theta + \tan^4\theta -$$

$$\left. - \frac{2}{\pi}\theta\tan^4\theta\right\}$$

All the static moment constants are zero since the center of moments is taken at the center of radius of the spherical cap. The simple C.G. transfer relatic ' ips of Section 3.2F and 4.2F can be used to obtain moments and moment derivatives about any other C.G. location. The force and moment coefficient constants are based on the base area (A_B) and base radius (R_B) of the bottom half of the spherical cap segment.

It is interesting to note that for a C.G. located at the center of radius of the spherical cap ($x_0 = R$, $z_0 = 0$) all the damping constants are zero as they should be. Since simple C.G. transfer relationships do not exist in general for the damping derivatives, the constants must be expressed in terms of the C.G. position.

For the case of a half sphere ($\theta = 0$), the static force coefficient constants assume an especially simple form

$$(K_A)_1 = (K_A)_3 = (K_N)_2 = (K_N)_3 = 1$$

$$(K_A)_2 = (K_N)_1 = \frac{1}{2}$$

$$(K_{Y\beta})_1 = (K_{Y\beta})_2 = -1$$

From these constants, it is possible to write an equation for C_A, C_N, and C_{Y_β} of the bottom of the half spherical cap at positive angles of attack.

$$C_A = \frac{3-\sqrt{5}}{4} + \frac{1}{2}\sqrt{5}\,\sin^2(58.28^\circ + \alpha) \qquad (5.1)$$

$$C_N = \frac{3-\sqrt{5}}{4} + \frac{1}{2}\sqrt{5}\,\sin^2(31.72^\circ + \alpha) \qquad (5.2)$$

$$C_{Y_\beta} = -\sqrt{2}\,\sin(45^\circ + \alpha) \tag{5.3}$$

From these equations it is easy to show that at $\alpha = 0$, $C_{Y_\beta} = -C_{N_\alpha}$, a not unexpected result.

5.3 Longitudinal Force Coefficients of a Blunt Cone

For the present, only equations for the longitudinal force coefficients of a blunt cone have been derived. The moments and damping derivatives, both longitudinal and lateral-direction, will be treated in the next quarter. In many respects the procedure is basically that which will be shown below. The primary additional complication is that static moments and damping derivatives of various parts of a composite configuration are a function of arm lengths or distance from the center of moments (C.G.) of the total configuration.

In order to derive the longitudinal force coefficients of a blunt cone, certain area relationships are required. These relationships are presented and explained with an appropriate diagram below.

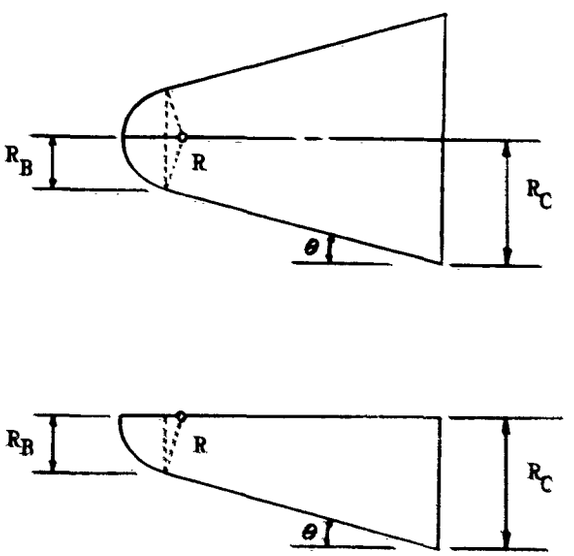

Diagram of a Blunt Circular Half Cone

The bluntness factor (f_B) of the cone will be defined in terms of the base radius of the cone (R_C) and the base radius of the spherical cap segment (R_B).

$$f_B = \left(\frac{R_B}{R_C}\right)^2 \tag{5.4}$$

The total planform area of the blunt cone (S) is composed of the truncated cone planform area (S_C) and the planform area of the spherical cap (S_B).

$$S = S_C + S_B \tag{5.5}$$

The cap force coefficients are based on the cap base area (A_B). The truncated cone force coefficients are based on the truncated cone planform area (S_C). If the blunt cone force coefficients are based on the total area (S), then the important area ratios, expressed in terms of the bluntness factor and the cone angle, are found to be the following:

$$\frac{A_B}{S} = \frac{\frac{\pi}{2}\left(\frac{f_B}{1-f_B}\right)\tan\theta}{1+\frac{\pi}{2}\left(\frac{f_B}{1-f_B}\right)\tan\theta\sec^2\theta\left[1-\frac{2}{\pi}\left(\theta+\frac{1}{2}\sin 2\theta\right)\right]} \tag{5.6}$$

$$\frac{S_C}{S} = \frac{1}{1+\frac{\pi}{2}\left(\frac{f_B}{1-f_B}\right)\tan\theta\sec^2\theta\left[1-\frac{2}{\pi}\left(\theta+\frac{1}{2}\sin 2\theta\right)\right]} \tag{5.7}$$

Based on total planform area, the axial force coefficient (C_A) and normal force coefficient (C_N) of the blunt cone can be written as

$$C_A = (C_A)_B\left(\frac{A_B}{S}\right) + (C_A)_C\left(\frac{S_C}{S}\right)$$

$$C_N = (C_N)_B\left(\frac{A_B}{S}\right) + (C_N)_C\left(\frac{S_C}{S}\right)$$

The subscripts B and C refer to the spherical cap and truncated cone respectively. In terms of the constants derived for the cone and the cap these equations become

$$C_A = \left[(K_A)_{1B}\cos^2\alpha + (K_A)_{2B}\sin^2\alpha + (K_A)_{3B}\sin\alpha\cos\alpha\right]\left(\frac{A_B}{S}\right) +$$

$$+\left[(K_A)_{1C}\cos^2\alpha + (K_A)_{2C}\sin^2\alpha + (K_A)_{3C}\sin\alpha\cos\alpha\right]\left(\frac{S_C}{S}\right)$$

$$C_N = \left[(K_N)_{1B}\cos^2\alpha + (K_N)_{2B}\sin^2\alpha + (K_N)_{3B}\sin\alpha\cos\alpha\right]\left(\frac{A_B}{S}\right) +$$

$$+\left[(K_N)_{1C}\cos^2\alpha + (K_N)_{2C}\sin^2\alpha + (K_N)_{3C}\sin\alpha\cos\alpha\right]\left(\frac{S_C}{S}\right)$$

One may define the composite or blunt cone constants as follows:

$$(K_A)_{1BC} = (K_A)_{1B}\left(\frac{A_B}{S}\right) + (K_A)_{1C}\left(\frac{S_C}{S}\right) \tag{5.8}$$

$$(K_A)_{2BC} = (K_A)_{2B}\left(\frac{A_B}{S}\right) + (K_A)_{2C}\left(\frac{S_C}{S}\right) \tag{5.9}$$

$$(K_A)_{3BC} = (K_A)_{3B}\left(\frac{A_B}{S}\right) + (K_A)_{3C}\left(\frac{S_C}{S}\right) \tag{5.10}$$

$$(K_N)_{1BC} = (K_N)_{1B}\left(\frac{A_B}{S}\right) + (K_N)_{1C}\left(\frac{S_C}{S}\right) \tag{5.11}$$

$$(K_N)_{2BC} = (K_N)_{2B}\left(\frac{A_B}{S}\right) + (K_N)_{2C}\left(\frac{S_C}{S}\right) \tag{5.12}$$

$$(K_N)_{3BC} = (K_N)_{3B}\left(\frac{A_B}{S}\right) + (K_N)_{3C}\left(\frac{S_C}{S}\right) \tag{5.13}$$

The C_A and C_N equations now become,

$$C_A = (K_A)_{1BC}\cos^2\alpha + (K_A)_{2BC}\sin^2\alpha + (K_A)_{3BC}\sin\alpha\cos\alpha \tag{5.14}$$

$$C_N = (K_N)_{1BC}\cos^2\alpha + (K_N)_{2BC}\sin^2\alpha + (K_N)_{3BC}\sin\alpha\cos\alpha \tag{5.15}$$

These equations for the blunt cone obviously take the same form as the equations for the sharp cone, or any other aerodynamic shape. The only difference is in the values of the constants. Eqs. (5.14) and (5.15) can also be expressed in the alternate and more useful form discussed in Section 3.3F.

$$C_A = (a_0)_{BC} + (a_1)_{BC}\sin^2\left[(\theta_a)_{BC} + \alpha\right] \tag{5.16}$$

$$C_N = (n_0)_{BC} + (n_1)_{BC}\sin^2\left[(\theta_n)_{BC} + \alpha\right] \tag{5.17}$$

where

$$(a_1)_{BC} = \sqrt{\left[(K_A)_{2BC} - (K_A)_{1BC}\right]^2 + (K_A)_{3BC}^2}$$

$$(a_0)_{BC} = \tfrac{1}{2}\left[(K_A)_{1BC} + (K_A)_{2BC}\right] - \tfrac{1}{2}(a_1)_{BC}$$

$$(\theta_a)_{BC} = \tfrac{1}{2}\tan^{-1}\frac{(K_A)_{3BC}}{(K_A)_{2BC} - (K_A)_{1BC}} = \tfrac{1}{2}\sin^{-1}\frac{(K_A)_{3BC}}{\sqrt{\left[(K_A)_{2BC} - (K_A)_{1BC}\right]^2 + (K_A)_{3BC}^2}}$$

$$(n_1)_{BC} = \sqrt{\left[(K_N)_{2BC} - (K_N)_{1BC}\right]^2 + (K_N)^2_{3BC}}$$

$$(n_0)_{BC} = \frac{1}{2}\left[(K_N)_{1BC} + (K_N)_{2BC}\right] - \frac{1}{2}(n_1)_{BC}$$

$$(\theta_n)_{BC} = \frac{1}{2}\tan^{-1}\frac{(K_N)_{3BC}}{(K_N)_{2BC} - (K_N)_{1BC}} = \frac{1}{2}\sin^{-1}\frac{(K_N)_{3BC}}{\sqrt{\left[(K_N)_{2BC} - (K_N)_{1BC}\right]^2 + (K_N)^2_{3BC}}}$$

It can easily be shown that the truncated cone constants based on planform area are the same as the constants for the sharp cone and can be obtained from Section 6.1F. The constants for the spherical cap are those shown in Section 5.2. Obviously it is possible with the procedure outlined to determine equations for C_A and C_N with numerical constants for any blunt half cone at positive angles of attack since the complete cone surface will "see" the flow. The procedure to be followed for the blunt full cone at all angles of attack is the same as that for sharp cones as discussed in Section 6.1F.

It is possible to obtain reasonably simple analytic expressions for the constants in Eqs. (5.16) and (5.17) if it is assumed that the half cone angle (θ) is small, and the bluntness factor (f_B) is also small. Retaining only up to third order terms in θ, f_B, and their products we have

$$(a_0)_{BC} = \left(\pi - \frac{8}{\pi}\right)\theta^3 + \frac{\pi}{2} f_B \theta\left(1 + \frac{3}{4} f_B - \frac{4}{\pi}\theta\right) \tag{5.18}$$

$$(a_1)_{BC} = \frac{\pi}{2}\theta\left[1 + \left(\frac{20}{\pi^2} - \frac{8}{3}\right)\theta^2\right] - \frac{\pi}{4} f_B \theta\left[1 - \pi\left(\frac{16}{\pi^2} - 1\right)\theta\right] \tag{5.19}$$

$$(\theta_a)_{BC} = \frac{4}{\pi}\theta\left[1+\left(\frac{7}{3}-\frac{64}{3\pi^2}\right)\theta^2\right] + \frac{1}{2}f_B\left[1+\frac{3}{2}f_B+\frac{4}{\pi}\theta+\frac{23}{12}f_B^2-\frac{2}{\pi}f_B\theta-\left(\frac{64}{\pi^2}-\frac{5}{2}\right)\theta^2\right] \quad (5.20)$$

$$(n_0)_{BC} = 2\left(1-\frac{3\pi^2}{32}\right)\theta^2 + \frac{\pi}{4}f_B\theta\left[1+f_B-\frac{3\pi}{4}\theta\right] \quad (5.21)$$

$$(n_1)_{BC} = \frac{4}{3}\left[1+\left(\frac{9\pi^2}{32}-\frac{5}{2}\right)\theta^2\right] - \frac{5\pi}{12}f_B\theta\left[1+f_B-\frac{9\pi}{10}\theta\right] \quad (5.22)$$

$$(\theta_n)_{BC} = \frac{3\pi}{8}\theta\left[1+\left(\frac{11}{6}-\frac{3\pi^2}{16}\right)\theta^2\right] + \frac{3\pi}{16}f_B\theta\left[1+f_B-\frac{3\pi}{8}\theta\right] \quad (5.23)$$

The initial terms, involving only the angle θ, are the values of the constants for the sharp cone. The terms containing f_B are the contributions of bluntness. These equations for the constants can be compared to the exact values computed numerically using Eq. (5.8) through Eq. (5.13). The exact values are plotted as a function of the cone half angle (θ) in Figs. 13 and 14. The approximate expressions for the constants will give good results for $f_B < .16$ and $\theta < 12^0$.

It should be possible to develop similar expressions for the moments and damping derivatives of the blunt cone. This will be discussed in some detail in a future report.

6.0 Hypersonic Pressure Relationships - Deviations from Newtonian

6.1 General Discussion

All of the work that has been done on stability derivatives up to this point has been based on the simple Newtonian pressure coefficient relationship at a point $C_p = 2\sin^2\delta$, where δ is the angle between the free stream flow and the plane tangent to the surface at the point. Under the assumptions of Newtonian flow, this equation applies only as long as $\delta > 0$.

For negative δ's , the pressure coefficient is assumed to be zero. In the strictest sense, the Newtonian pressure relationship applies only as $M \rightarrow \infty$, and the gas constant γ is assumed to be one. In a practical sense, the Newtonian relationship appears generally to give reasonable results for the total forces as long as $M\delta > 4.0$, and the body is highly three-dimensional, such as a cone. For the negative pressure region of the body $|M\delta| > 4.0$, the negative pressures are less than 5 percent of the Newtonian positive pressures, and therefore can be safely neglected.

An alternative to the Newtonian constant 2 has been suggested which gives better results for the pressures on blunt noses. The relationship is of the form

$$C_p = K \sin^2\delta \tag{6.1}$$

Where the constant K is taken as the stagnation pressure coefficient behind a normal shock.

Any pressure relationship of this form, that can be assumed to apply for the entire body at all values of $M\delta$, leads to no special problems. All of that which has been done on the stability derivatives assuming the Newtonian constant 2, is equally valid for any other value of K. The only requirement is that the equations for force and moment coefficients and stability derivatives must be multiplied by the ratio K/2.

It has been established that the pressure coefficients of similar bodies can be related to one another at hypersonic speeds through the similarity parameter $M\delta$. But for different body shapes, no such simple relationship exists. In a strict sense, the constant K in Eq. (6.1) that is applicable at any point on the body is not only a function of the local value of $M\delta$, but is also a more complicated function of the general body geometry. The pressures behind a blunt nose, for example, are a function of the bluntness as well as the local value of $M\delta$. A flat plate delta wing at angle of attack with constant free stream $M\delta$, has a pressure coefficient which in general varies along the span.

Obviously the problem of computing pressures at hypersonic speeds on surfaces, and integrating the results to obtain the stability derivatives, is an extremely complex one. A first approach to this problem is to consider those configurations which obviously have uniform pressures everywhere, and try to establish the proper pressure relations as a function of only the hypersonic similarity parameter ($M\delta$). One such configuration is the circular cone at zero angle of attack, another is the two-dimensional flat plate at angle of attack. For the present, only those conditions with nose and leading edge shocks attached will be considered. The Newtonian pressure coefficient relationship, Eq. (6.1), and the combined hypersonic-supersonic similarity law suggest that the form the pressure coefficient might take is

$$\frac{C_p}{\sin^2\delta} = g(\beta \sin\delta) \tag{6.2}$$

where

δ = angle between the surface and free stream

$$\beta = \sqrt{M^2 - 1}$$

For sufficiently high Mach numbers and small δ's, Eq. (6.2) will reduce to the form

$$\frac{C_p}{\delta^2} = g(M\delta) \tag{6.3}$$

Obviously the assumptions of Newtonian flow, γ 1.0 and $M \to \infty$, are such that $g(\beta \sin\delta) = 2$.

Eq. (6.2) has some interesting implications in the light of the force and moment coefficient and stability derivative equations that have been derived assuming Newtonian flow. All of these results have shown that the force and moment coefficients are a function of a parameter of the form $\sin^2(\theta_x + \alpha)$, and the derivatives are a function of $\sin(\theta_x + \alpha)$. The angle θ_x can be considered

to be an average integrated surface angle, or the "effective" surface angle which varies with the surface shape and the force coefficient or derivative being evaluated. In the light of Eq. (6.2), it may be possible to consider that for the entire surface being analyzed, the average δ is $(\theta_x+\alpha)$. If this is possible, then the surface average pressure law that is applicable is obtained by simple substitution in Eq. (6.2)

$$\frac{C_p}{\sin^2(\theta_x+\alpha)} = g\left[\beta \sin(\theta_x+\alpha)\right] \tag{6.4}$$

If evaluation of Eq. (6.4) results in a number different than the Newtonian 2, the implication is that the computed Newtonian results for the force and moment coefficients and stability derivatives at $(\theta_x+\alpha)$ should be multiplied by the following ratio:

$$\frac{g\left[\beta \sin(\theta_x+\alpha)\right]}{2}$$

Of course this procedure is all predicated on the fact that Eq. (6.2) is applicable on the average to the shape under consideration.

At some hypersonic speeds and angles of attack, negative pressures on a body are far from negligible. If an applicable equation, similar to Eq. (6.2) can be derived for expansion angles (δ_e), then it may be possible to account for the negative pressures that are neglected in the simple Newtonian theory. For negative pressures Eq. (6.2) becomes

$$\frac{C_p}{\sin^2\delta_e} = g'(\beta \sin\delta_e) \tag{6.5}$$

It has been established that within limits, the function $g'(\beta \sin \delta_e)$ can certainly be evaluated for Prandtl-Meyer expansion on a two-dimensional flat plate at hypersonic velocities. Whether similar relationships are possible on other shapes has not as yet been determined.

Eq. (6.5) also has interesting implications in light of what has been done in Newtonian flow. When the angle ($\theta_x + \alpha$) for the bottom surface or the angle ($\theta_x - \alpha$) for the top surfaces becomes negative, the procedure has been to drop the negative angle term completely in determining force and moment coefficients and stability derivatives. Eq. (6.5) establishes a possible method for considering such negative pressures following a procedure identical to that used for positive pressures. Thus the possibility exists that the Newtonian results can be corrected, at least approximately, to account for negative pressures on the basis of the "effective" negative angle ($\theta_x \pm \alpha$) of the surface, where

$$\delta_e = (\theta_x + \alpha) \text{ for the bottom when } \quad \alpha < -\theta_x$$

$$\delta_e = (\theta_x - \alpha) \text{ for the top when } \quad \alpha > \theta_x$$

The procedures suggested above for correcting the Newtonian stability derivatives is by no means a rigorous one. It will of course be checked by comparing results with actual experimental data. For this procedure to be fruitful, appropriate relationships of the form of Eq. (6.2) and (6.5) must be found. This approach is only a beginning, and as the program progresses other methods will also be investigated.

6.2 Pressure Laws at Hypersonic Velocities

The present discussion will be concerned with methods available for establishing the functional relationships indicated by Eq. (6.2) and Eq. (6.5) at hypersonic velocities.

For the two dimensional case, oblique shock and Prandtl-Meyer expansion, the functional relationships of Eqs. (6.2) and (6.5), with certain restrictions, have been established and appear in the literature in various analytic forms.

Under the assumption that the shock angle and wedge angle (δ) are small, say $\delta < 10^\circ$, and $M > 4.5$, it is possible to establish a very simple expression for the pressure coefficient of the wedge, which takes the form

$$\frac{C_p}{\delta^2} = \frac{\gamma+1}{2} + \sqrt{\left(\frac{\gamma+1}{2}\right)^2 + \frac{4}{(M\delta)^2}} \quad . \tag{6.6}$$

Assuming γ to be constant, the only variable on the right hand side of the equation is the hypersonic similarity parameter, $M\delta$. Eq. (6.6) can be expanded in various power series that give good results for particular ranges of $M\delta$. These expressions are shown below.

<u>$M\delta < 1.40$</u>

$$\frac{C_p}{\delta^2} = \frac{2}{M\delta} + \left(\frac{\gamma+1}{2}\right) + \left(\frac{\gamma+1}{4}\right)^2 M\delta \tag{6.7}$$

<u>$1.0 < M\delta < 2.60$</u>

$$\frac{C_p}{\delta^2} = \frac{\frac{3}{2}\sqrt{2}}{M\delta} + \left(\frac{\gamma+1}{2}\right) + \frac{1}{2}\sqrt{2}\left(\frac{\gamma+1}{4}\right)^2 M\delta \tag{6.8}$$

<u>$M\delta > 2.0$</u>

$$\frac{C_p}{\delta^2} = (\gamma+1) + \frac{4}{(\gamma+1)(M\delta)^2} \tag{6.9}$$

All of these equations give results with less than about 2 percent error in the ranges specified, and can be checked by comparison with the plot of Eq. (6.6) on Fig. 15. It is obvious from this plot that two-dimensional pressures are much higher than those predicted by the simple Newtonian equation at the lower values of $M\delta$.

Similar expressions can be established for Prandtl-Meyer expansion at hypersonic speeds. For expansion from free stream Mach Number (M) through a negative angle δ_e , the pressure coefficient in two-dimensional flow can be expressed as

$$\frac{C_p}{\delta_e^2} = \frac{2}{\gamma(M\delta_e)^2}\left\{\left[1+\left(\frac{\gamma-1}{2}\right)(M\delta_e)\right]^{\frac{2\gamma}{\gamma-1}} - 1\right\} \tag{6.10}$$

The only important assumption required for Eq. (6.10) to be valid is that the free stream Mach Number be reasonably large, say M > 4.5. Various simplified expressions can be derived from Eq. (6.10) that are valid over limited ranges of the expansion similarity parameter ($M\delta_e$). These expressions are listed below.

$|M\delta_e| < .50$

$$\frac{C_p}{\delta_e^2} = \frac{2}{M\delta_e} + \left(\frac{\gamma+1}{2}\right) + \left(\frac{\gamma+1}{6}\right) M\delta_e \tag{6.11}$$

$.40 < |M\delta_e| < 2.2$

$$\frac{C_p}{\delta_e^2} = -\frac{.0457}{(M\delta_e)^2} + \frac{1.807}{M\delta_e} + .885 + .1640(M\delta_e) \tag{6.12}$$

$|M\delta_e| > 2.0$

$$\frac{C_p}{\delta_e^2} = -\frac{2}{\gamma(M\delta_e)^2} \tag{6.13}$$

It is interesting to note that Eq. (6.11) differs only slightly from Eq. (6.7). The constant in the last term is about 10 percent larger for a γ of 1.4. Eq. (6.10) is plotted as Fig. 16, and the accuracies of Eqs. (6.11), (6.12), and (6.13) can be determined by direct comparison.

Comparison of Figs. 15 and 16 indicates that at small values of $M\delta$, $M\delta = |M\delta_e| \leq .10$, expansion and compression effects are equally as important in determining forces and moments on a body. At $M\delta = |M\delta_e| = 1.0$, compression effects are approximately three times as great. At $M\delta = |M\delta_e| = 5.0$, the

expansion effects are negligible.

The relationships discussed so far are two-dimensional, and most shapes of interest in hypersonic flow are in general quite three-dimensional. A three-dimensional shape that has been analyzed in some detail at zero angle of attack is the cone. Cone pressure coefficients computed by the Taylor-Maccoll theory have been tabulated by Kopal (Ref. 1). This data, for cone semi-angles of less than 10^0 is plotted as a function of the similarity parameter $\beta\delta$ in Fig. 15.

Several explicit analytic solutions for the pressures on a cone have been determined and exist in the literature. A simple solution for a slender cone in supersonic flow is

$$\frac{C_p}{\delta^2} = 2 \ln \frac{2}{\beta\delta} - 1 \tag{6.14}$$

This has only very limited applicability. A comparison of Eq. (6.14) with the results of Fig. 15 show that it is applicable only for $\beta\delta < 0.1$. A second order approximation for the pressure on a cone at zero angle of attack was determined by Broderick (Ref. 2).

$$C_p = -\delta^2 + 2\delta^2 \ln \frac{2}{(M^2-1)^{1/2}\delta} + 5(M^2-1)\delta^4 \left[\ln \frac{2}{(M^2-1)^{1/2}\delta}\right]^2 -$$

$$-(5M^2-1)\delta^4 \ln \frac{2}{(M^2-1)^{1/2}\delta} + \delta^4\left[\frac{13}{4}M^2 + \frac{1}{2} + \frac{(\gamma+1)M^4}{(M^2-1)}\right] \tag{6.15}$$

For small angle cones ($\delta < 10^0$), and M larger than 2, the above equation can be simplified and made a function of only the similarity parameter ($\beta\delta$).

$$\frac{C_p}{\delta^2} = \left[\left(\frac{4\gamma+17}{4}\right)(\beta\delta)^2 - 1\right] + \left[2 - 5(\beta\delta)^2 + 5(\beta\delta)^2 \ln \frac{2}{(\beta\delta)}\right] \ln \frac{2}{(\beta\delta)} \tag{6.16}$$

This equation can be compared to the Kopal results of Fig. 15. The comparison is good for $\beta\delta < .50$.

Cole's hypersonic slender body theory makes it possible to determine second order approximations to the surface pressures on slender bodies. The second order approximation is essentially a correction to the first order approximation, which consists of simple Newtonian plus centrifugal forces. The second order hypersonic solution for the pressure on the cone at zero angle of attack is

$$\frac{C_p}{\delta^2} = \frac{5\gamma+3}{2(\gamma+1)} + \frac{1}{2(M\delta)^2} \qquad (6.17)$$

Eq. (6.17) checks quite well with the Kopal results shown in Fig. 15 for $\beta\delta > 1.5$.

It becomes obvious from the two-dimensional and cone results presented, that geometry has an especially strong influence on the magnitude of the pressures experienced by a body in hypersonic flow at low values of the similarity parameter. At $\beta\delta$ or $M\delta$ of 0.1, the pressure on a slender cone is only 1/4 of the two-dimensional value. At higher values of $M\delta$, say $M\delta = 5.0$, the cone pressures is only 13 percent less than the two-dimensional result. It is also true that under these conditions both cone and two-dimensional pressures do not differ greatly from simple Newtonian.

The cone pressure results shown here will be used to determine Mach Number corrections to force and moment coefficients and stability derivatives for the cone that have been determined assuming simple Newtonian theory. By comparing these results to experimental data, the degree of validity of the approach suggested in Section 6.1 will be established.

An investigation of other body shapes is obviously required in order to bridge the gap between the pressures on a two-dimensional wedge and a three-dimensional cone. But second order solutions on other than bodies of revolution at zero angle of attack are difficult to obtain. A second order solution has been obtained on a delta planform with diamond shape cross-section (Ref. 3), and these results will be investigated further.

The discussion up to this point has been concerned with corrections to the Newtonian results for small angles of attack with attached shocks. A similar problem exists at larger angles of attack where the shock may actually be detached. The investigation of this problem will also be undertaken.

7.0 Projected Work - Third Quarter

During the next quarter, many of the results shown in this report for the force and moment coefficients and stability derivative equations in Newtonian flow will be extended. Specifically the investigation into the stability derivatives of the sharp elliptic cone will be continued. The work on the stability derivatives of the blunt cone will also be extended. As explained in the "First Quarterly Technical Report", the purpose in these investigations is to show the application of the general methods derived rather than a detailed investigation of specific families of shapes.

A beginning has been made in this report on the application of other hypersonic theories to the prediction of stability derivatives. This investigation will continue. In Section 6.1 a tentative procedure has been outlined for extending the Newtonian results to lower hypersonic Mach numbers. This procedure will be applied to the cone, and possibly other shapes, and the results compared to existing experimental data.

During the next quarter, a concentrated effort will be made to develop methods for computing the stability derivatives under trim conditions, a primary goal in this whole hypersonic stability investigation. The basic methods and procedures presented in this and the previous quarterly report lay the groundwork for this investigation. The first shape to be investigated under trim conditions will be the delta-planform with diamond-shape cross-section, since this will be easiest to treat. The controls to be used for trim will probably be a trailing edge deflected flap. To the degree possible, stability derivatives with trim will also be investigated on the circular and elliptic cone.

The discussion up to this point has been concerned with corrections to the Newtonian results for small angles of attack with attached shocks. A similar problem exists at larger angles of attack where the shock may actually be detached. The investigation of this problem will also be undertaken.

7.0 Projected Work - Third Quarter

During the next quarter, many of the results shown in this report for the force and moment coefficients and stability derivative equations in Newtonian flow will be extended. Specifically the investigation into the stability derivatives of the sharp elliptic cone will be continued. The work on the stability derivatives of the blunt cone will also be extended. As explained in the "First Quarterly Technical Report", the purpose in these investigations is to show the application of the general methods derived rather than a detailed investigation of specific families of shapes.

A beginning has been made in this report on the application of other hypersonic theories to the prediction of stability derivatives. This investigation will continue. In Section 6.1 a tentative procedure has been outlined for extending the Newtonian results to lower hypersonic Mach numbers. This procedure will be applied to the cone, and possibly other shapes, and the results compared to existing experimental data.

During the next quarter, a concentrated effort will be made to develop methods for computing the stability derivatives under trim conditions, a primary goal in this whole hypersonic stability investigation. The basic methods and procedures presented in this and the previous quarterly report lay the groundwork for this investigation. The first shape to be investigated under trim conditions will be the delta-planform with diamond-shape cross-section, since this will be easiest to treat. The controls to be used for trim will probably be a trailing edge deflected flap. To the degree possible, stability derivatives with trim will also be investigated on the circular and elliptic cone.

List of References

1. Kopal, Zdenek, "Tables of Supersonic Flow Around Cones", M.I.T. Technical Report No. 1, 1947.

2. Broderick, J.B., "Supersonic Flow Round Pointed Bodies of Revolution", Quart. Jour. Mech. and Applied Math., Vol. II, Pt. 1, 1949.

3. Tan, H.S., "Second Approximation to Conical Flows", Cornell University Contract No. AF 33 (038) -9832, Dec. 1950. ATI Report 95185.

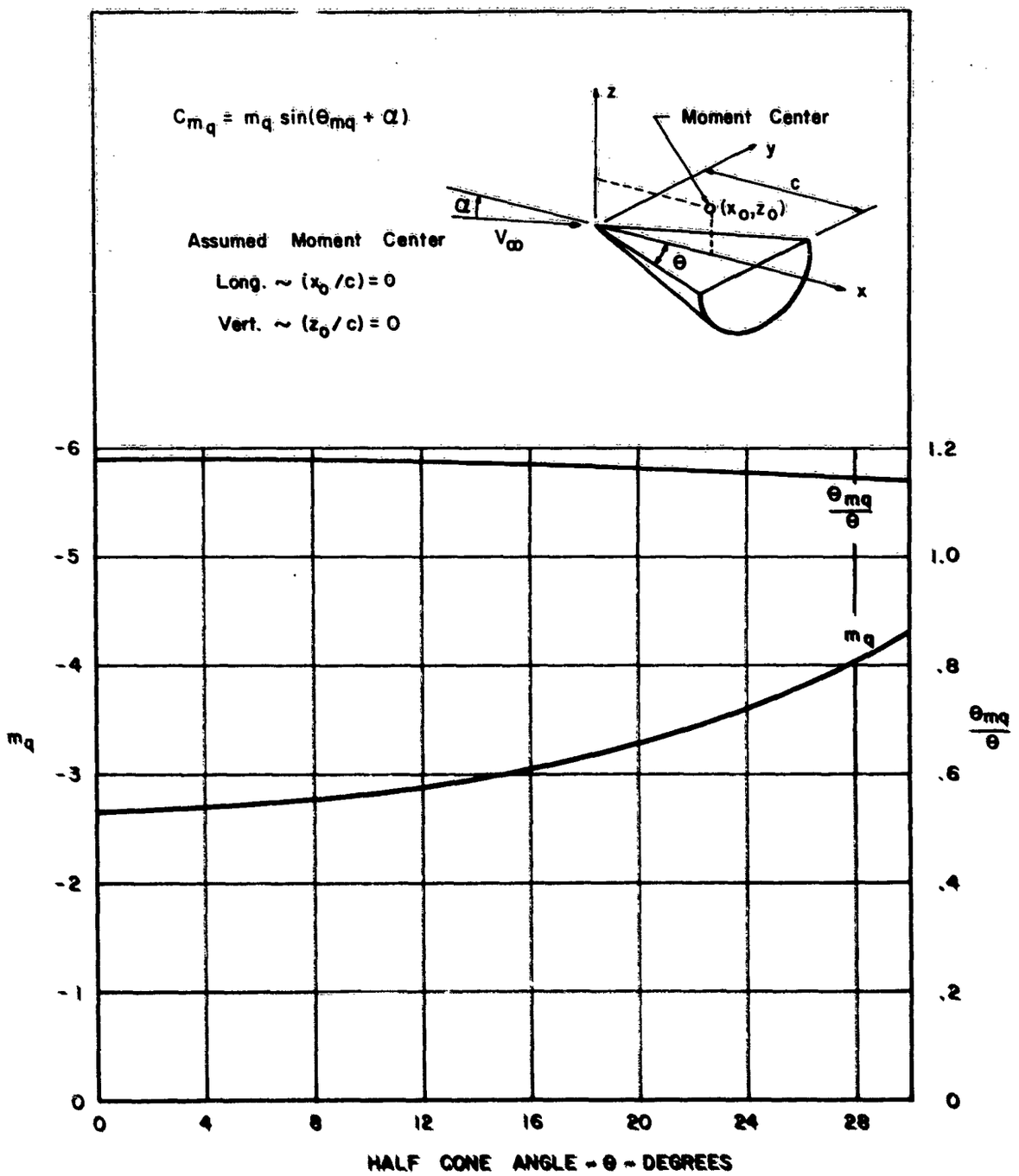

FIGURE 1. NEWTONIAN CONSTANTS FOR A HALF CIRCULAR CONE
DAMPING IN PITCH - C.G. AT $(x_0/c) = 0$, $(z_0/c) = 0$
CONDITIONS: $\alpha \geq -\theta$, $\beta = 0$, $\phi = 0$

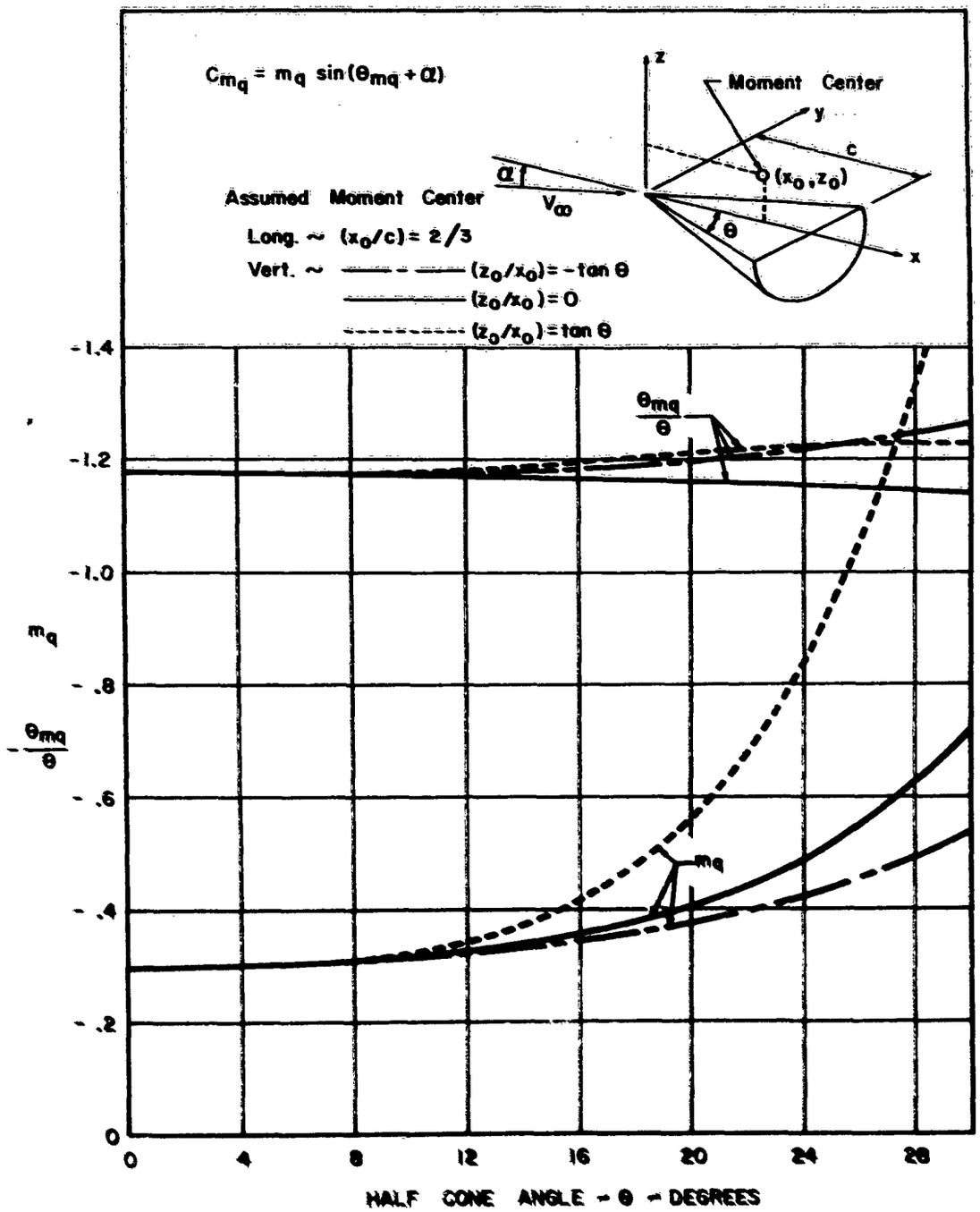

FIGURE 2. NEWTONIAN CONSTANTS FOR A HALF CIRCULAR CONE
DAMPING IN PITCH - C.G. AT $(x_0/c) = 2/3$, (z_0/x_0) VARIES
CONDITIONS: $\alpha \geq -\theta$, $\beta = 0$, $\phi = 0$

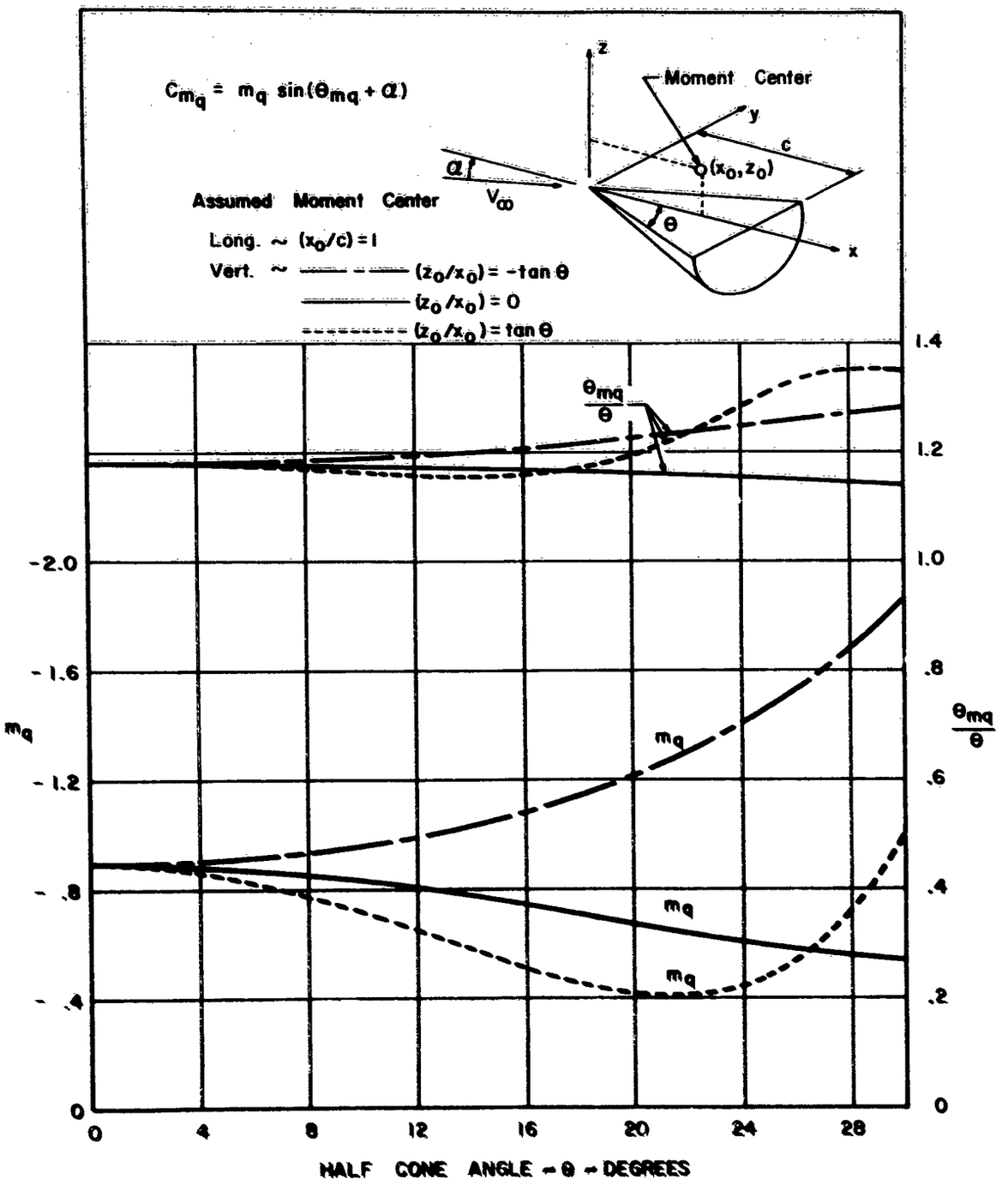

FIGURE 3. NEWTONIAN CONSTANTS FOR A HALF CIRCULAR CONE
DAMPING IN PITCH - C.G. AT $(x_0/c) = 1$, (z_0/x_0) VARIES
CONDITIONS $\alpha \geq -\theta$, $\beta = 0$, $\phi = 0$

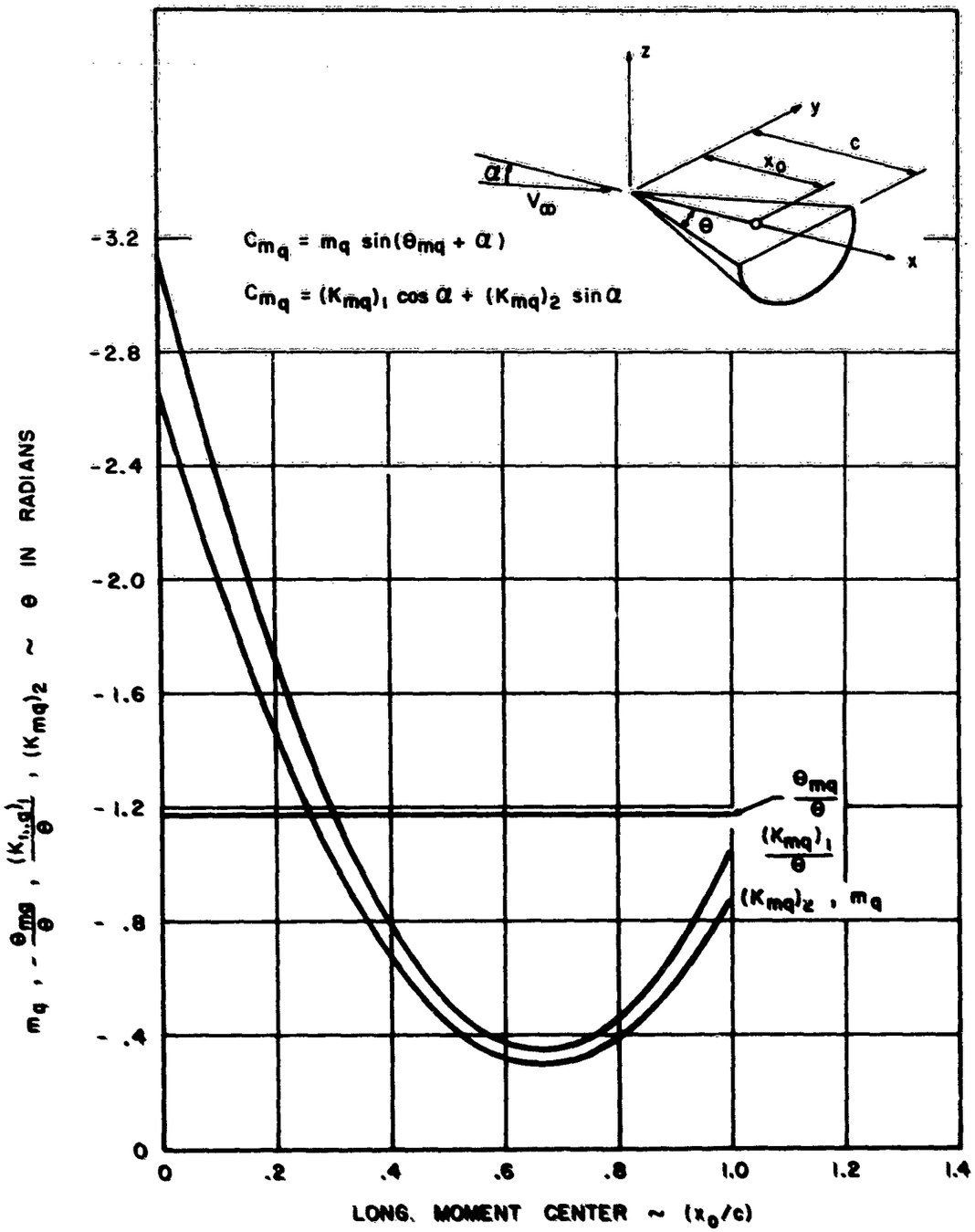

FIGURE 4. NEWTONIAN CONSTANTS FOR A HALF CIRCULAR CONE
DAMPING IN PITCH OF A SLENDER CONE

CONDITIONS: $\alpha \geq -\theta$, $\beta = 0$, $\phi = 0$

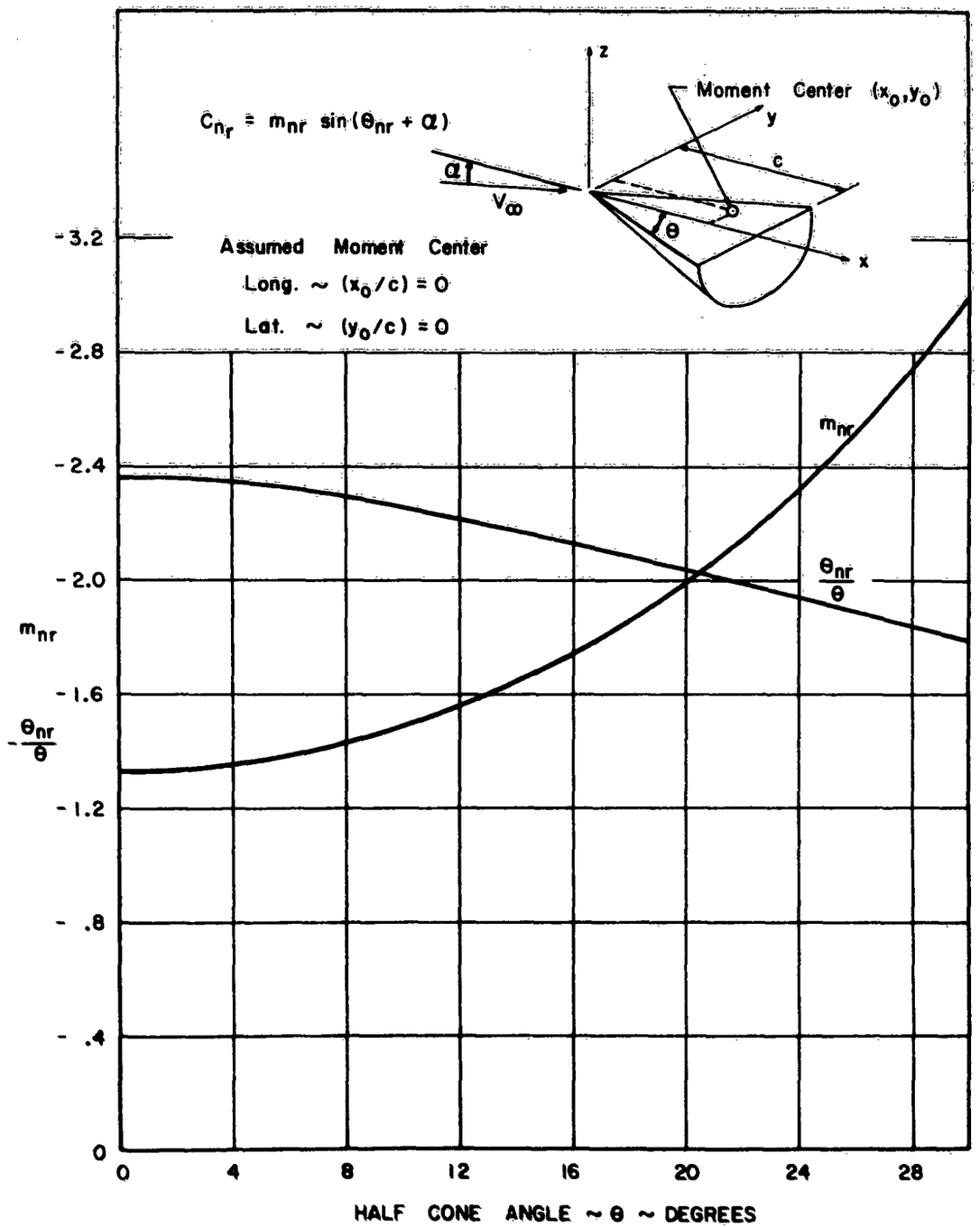

FIGURE 5. NEWTONIAN CONSTANTS FOR A HALF CIRCULAR CONE DAMPING IN YAW - C.G. AT $(x_o/c) = 0$, $(y_o/c) = 0$

CONDITIONS: $\alpha \geq -\theta$, $\beta = 0$, $\phi = 0$

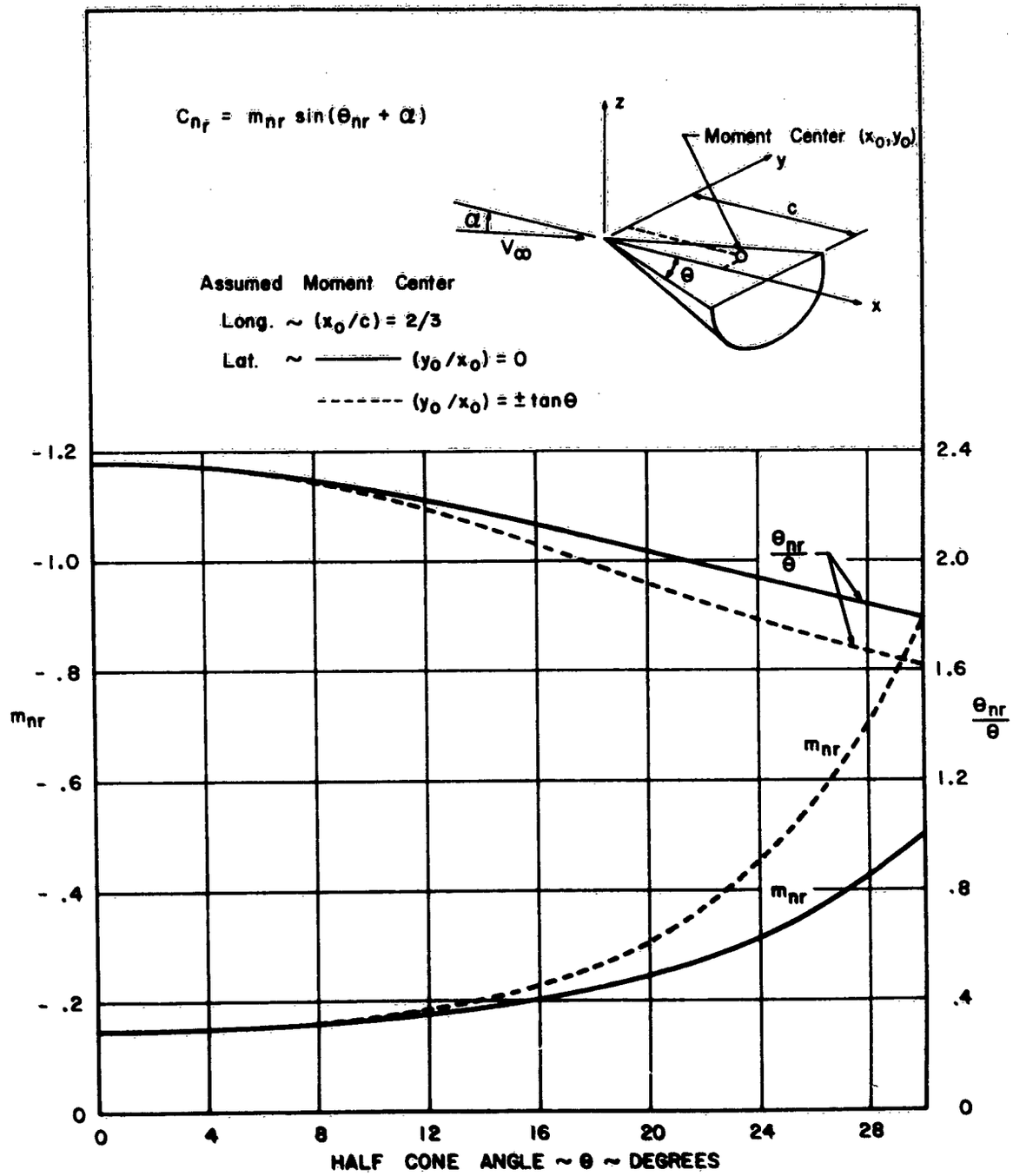

FIGURE 6. NEWTONIAN CONSTANTS FOR A HALF CIRCULAR CONE
DAMPING IN YAW - C.G. AT $(x_0/c) = 2/3$, (y_0/x_0) VARIES

CONDITIONS: $\alpha \geq -\theta$, $\beta = 0$, $\phi = 0$

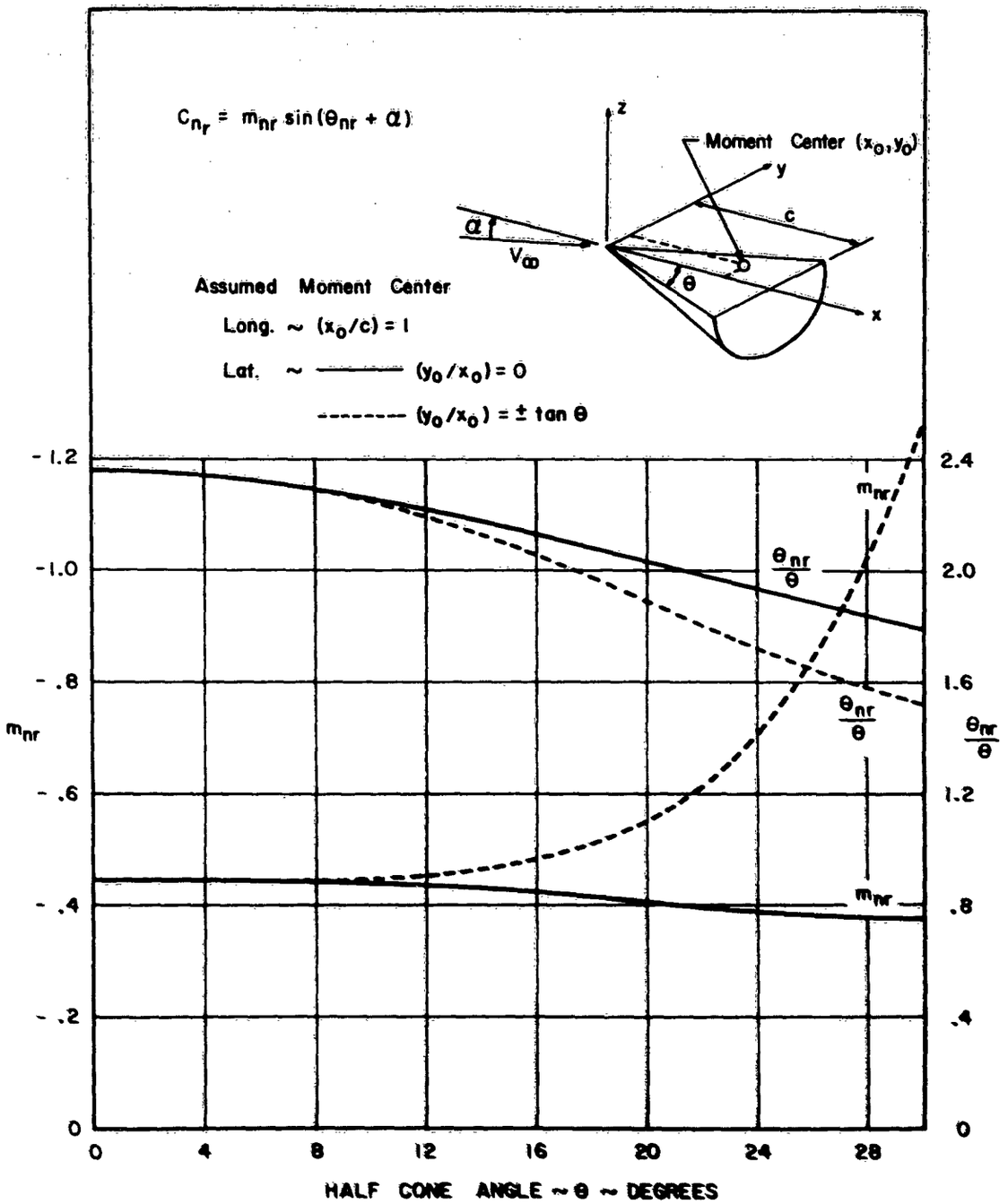

FIGURE 7. NEWTONIAN CONSTANTS FOR A HALF CIRCULAR CONE DAMPING IN YAW - C.G. AT $(x_o/c) = 1$, (y_o/x_o) VARIES

CONDITIONS: $\alpha \geq -\theta$, $\beta = 0$, $\phi = 0$

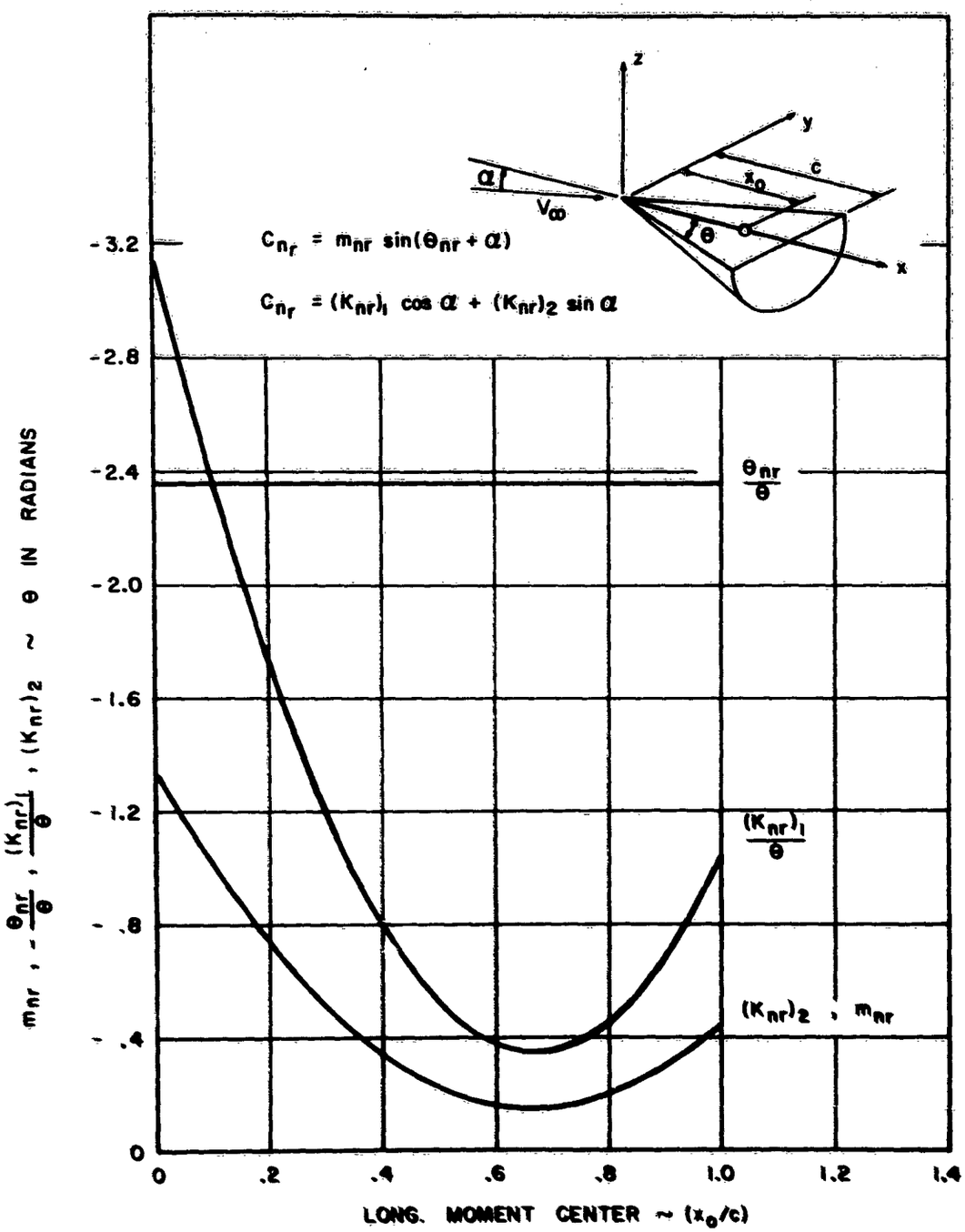

FIGURE 8. NEWTONIAN CONSTANTS FOR A HALF CIRCULAR CONE DAMPING IN YAW OF A SLENDER CONE

CONDITIONS: $\alpha \geq -\theta$, $\beta = 0$, $\phi = 0$

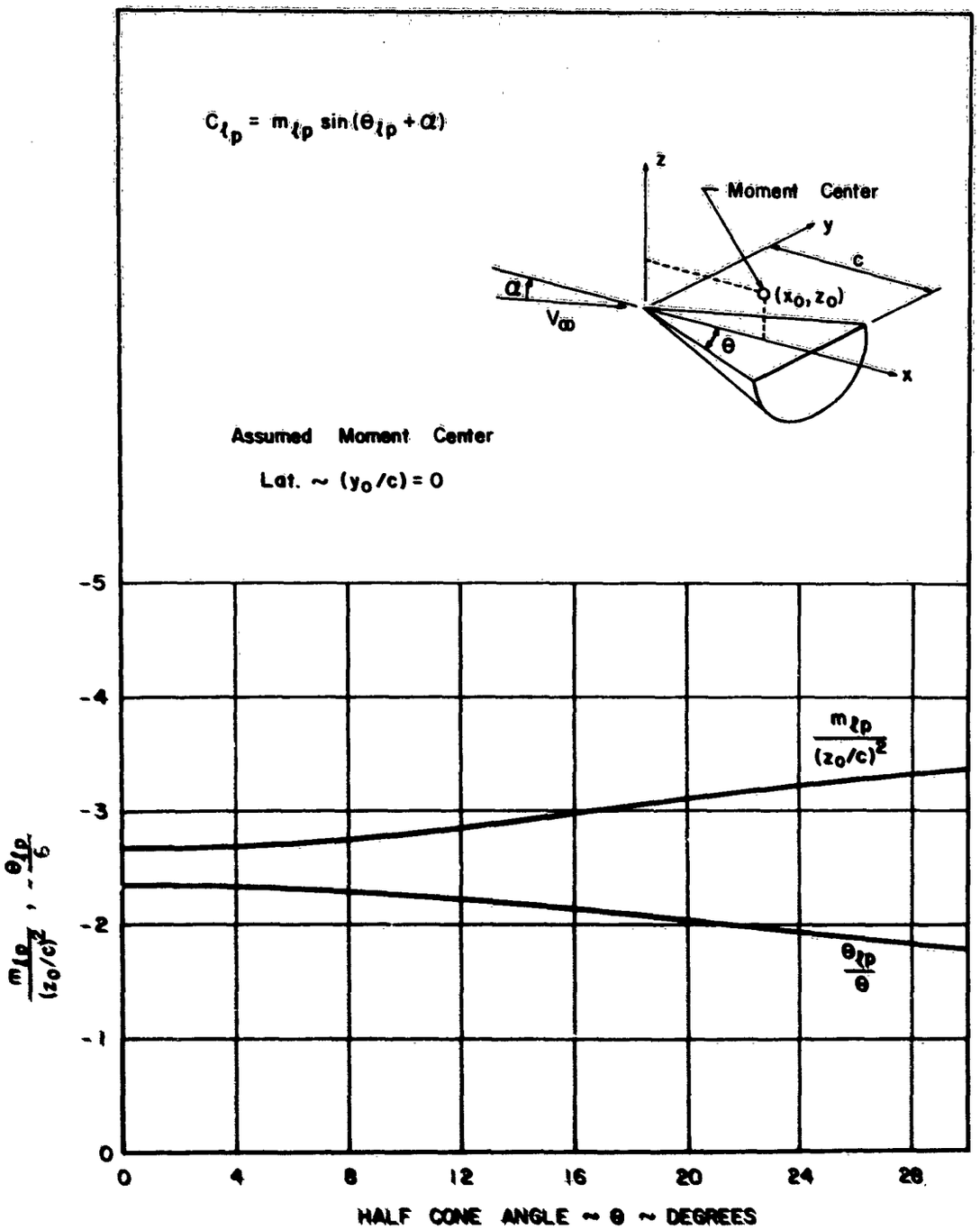

FIGURE 9. NEWTONIAN CONSTANTS FOR A HALF CIRCULAR CONE DAMPING IN ROLL - C.G. AT $(y_0/c) = 0$, (z_0/c) VARIES

CONDITIONS: $\alpha \geq -\theta$, $\beta = 0$, $\phi = 0$

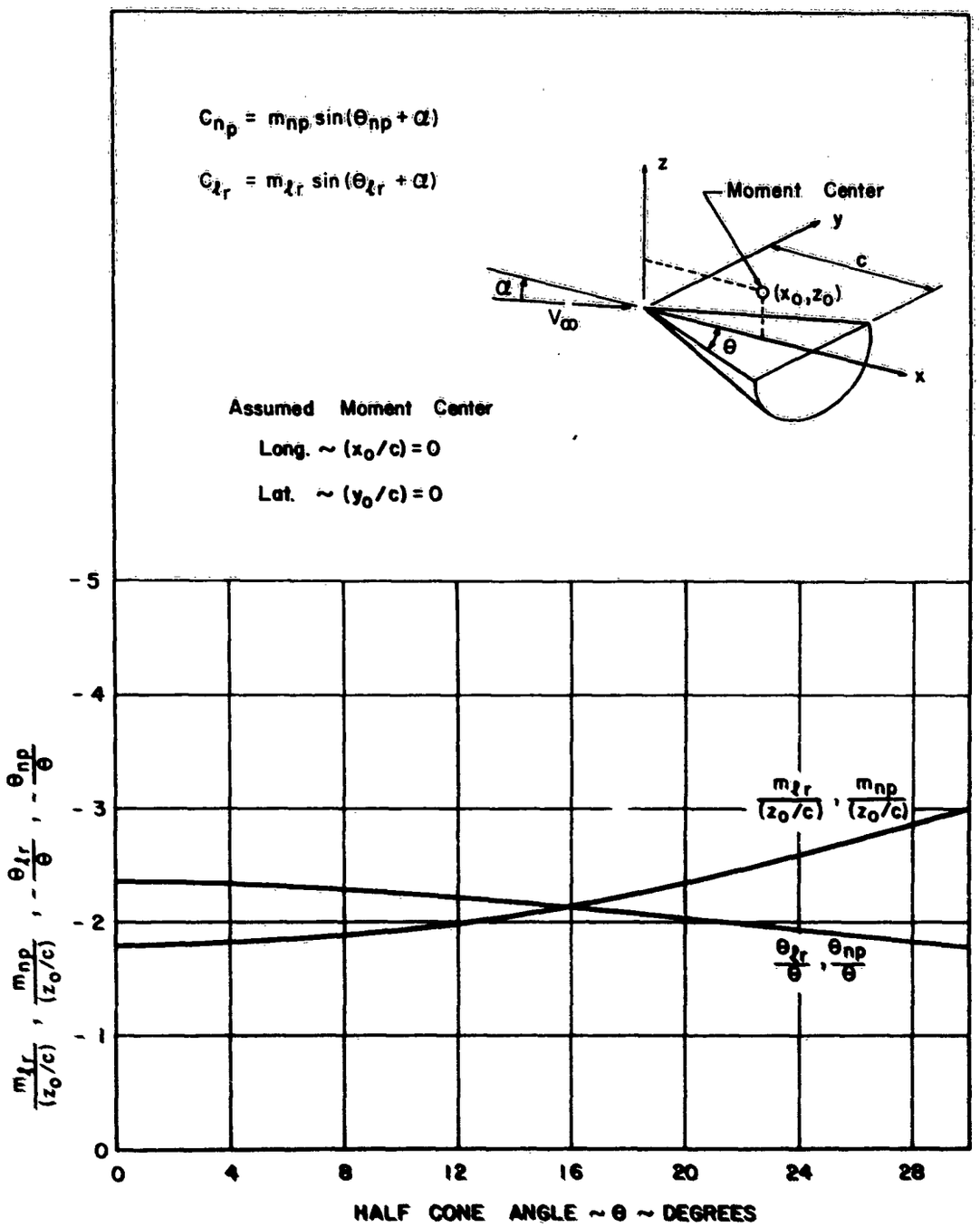

FIGURE 10. NEWTONIAN CONSTANTS FOR A HALF CIRCULAR CONE
DAMPING IN YAW DUE TO ROLLING AND ROLL DUE TO YAWING
C.G. AT $(x_0/c) = 0$, $(y_0/c) = 0$, (z_0/c) VARIES
CONDITIONS: $\alpha \geq -\theta$, $\beta = 0$, $\phi = 0$

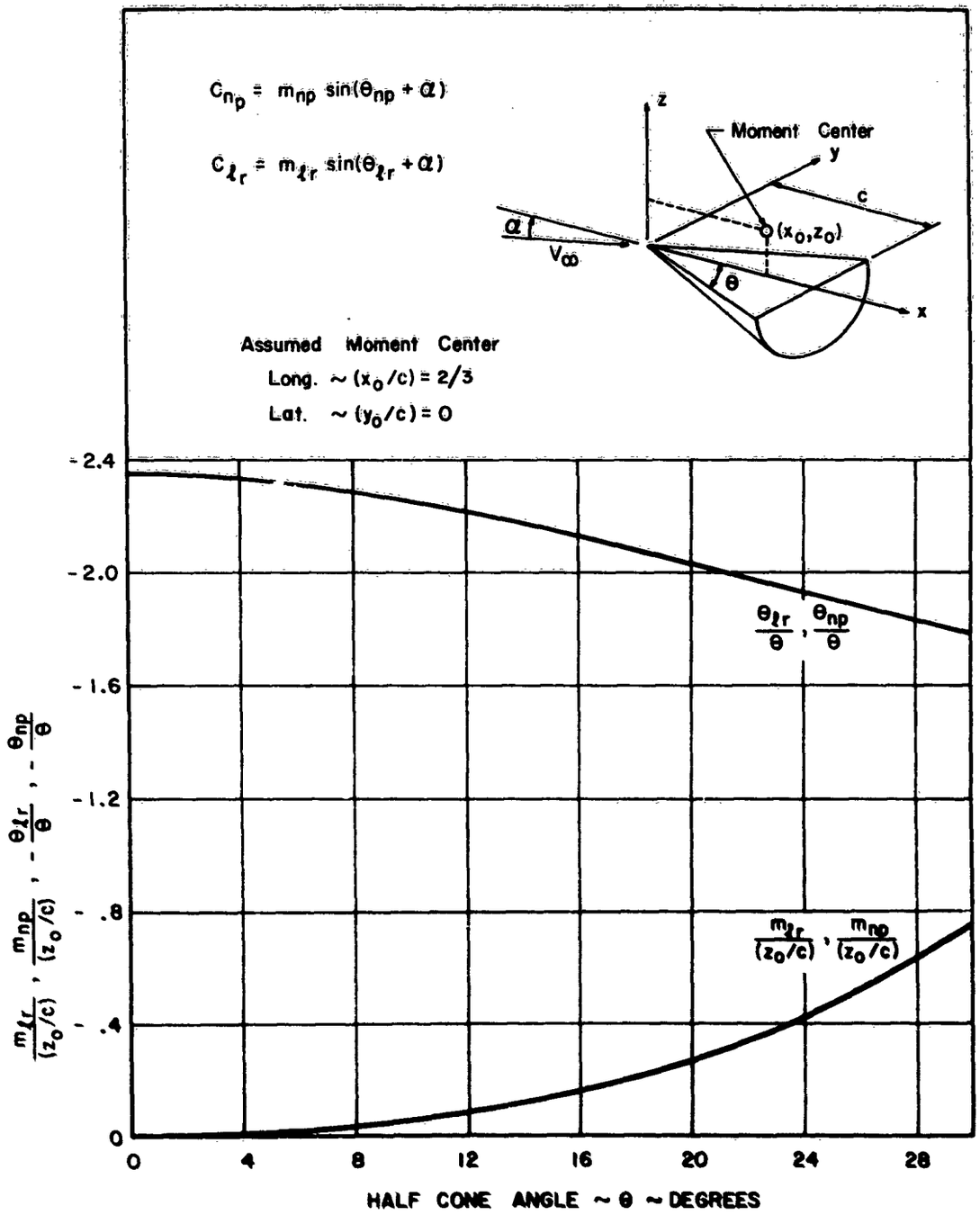

FIGURE 11. NEWTONIAN CONSTANTS FOR A HALF CIRCULAR CONE
DAMPING IN YAW DUE TO ROLLING AND ROLL DUE TO YAWING
C.G. AT $(x_0/c) = 2/3$, $(y_0/c) = 0$, (z_0/c) VARIES
CONDITIONS: $\alpha \geq -\theta$, $\beta = 0$, $\phi = 0$

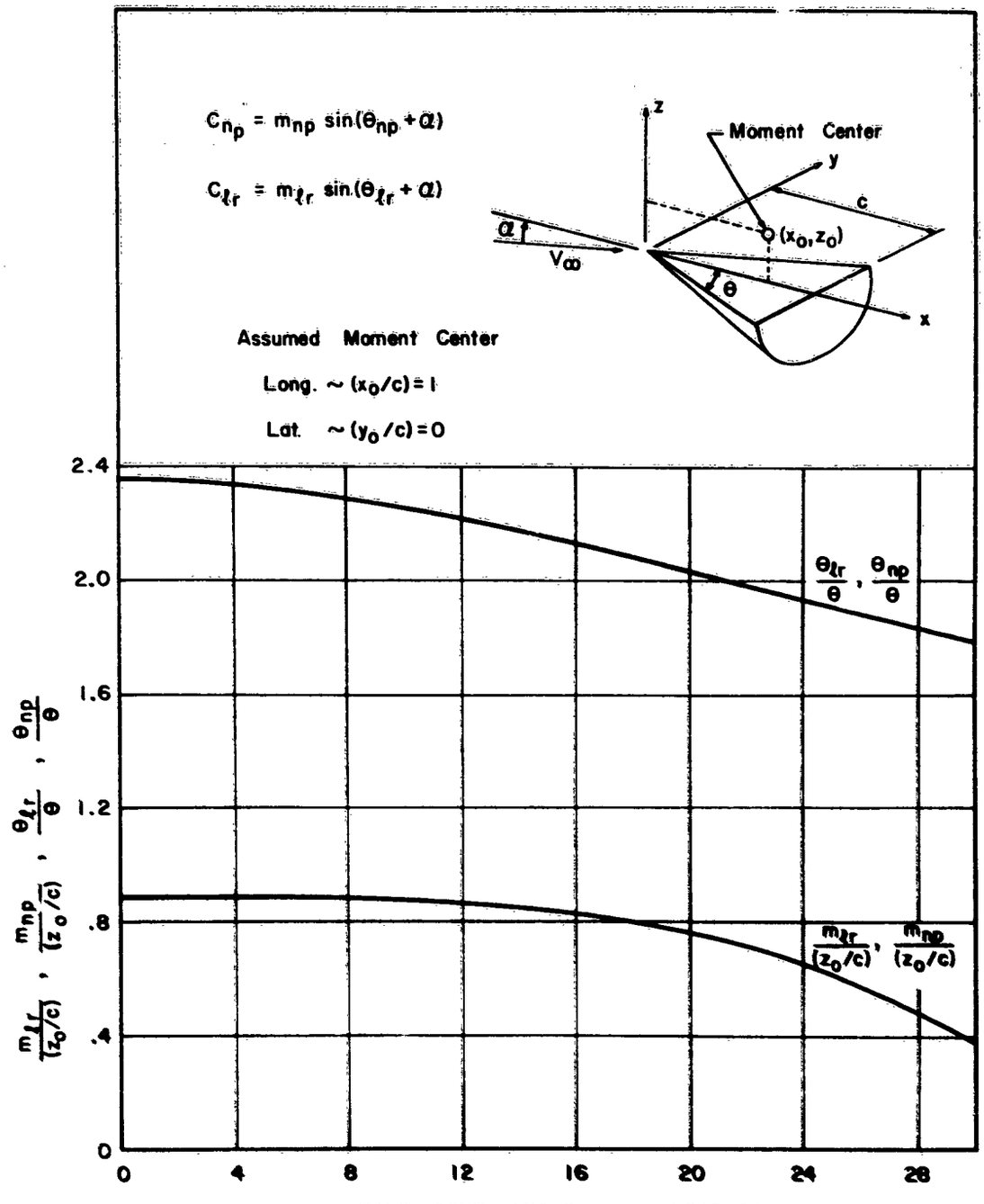

FIGURE 12. NEWTONIAN CONSTANTS FOR A HALF CIRCULAR CONE
DAMPING IN YAW DUE TO ROLLING AND ROLL DUE TO YAWING
C.G. AT $(x_0/c) = 1$, $(y_0/c) = 0$, (z_0/c) VARIES
CONDITIONS: $\alpha \geq -\theta$, $\beta = 0$, $\phi = 0$

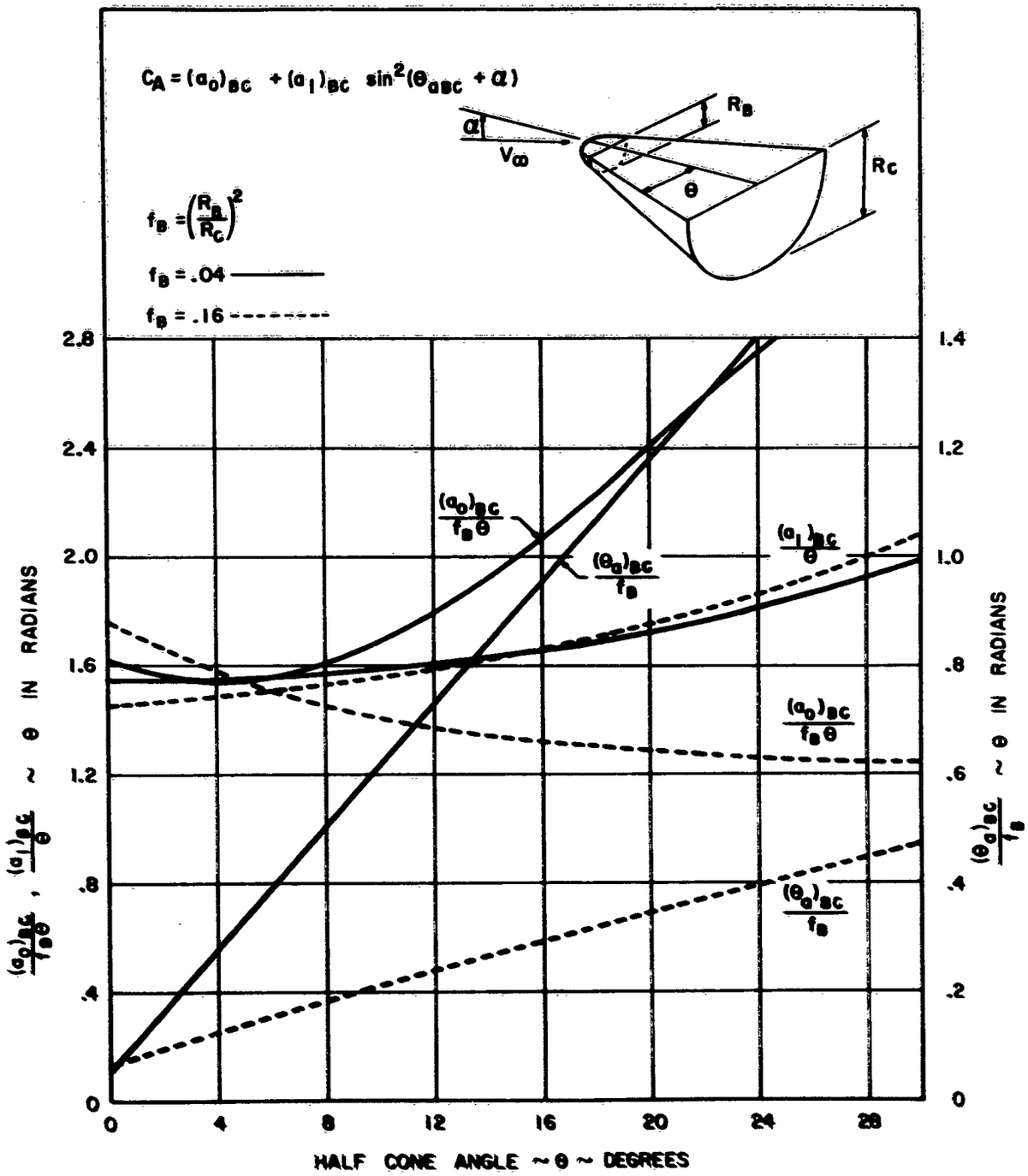

FIGURE 13. NEWTONIAN CONSTANTS FOR A BLUNT CIRCULAR HALF CONE AXIAL FORCE COEFFICIENT

CONDITIONS: $\alpha \geq -\theta$, $\beta = 0$, $\phi = 0$

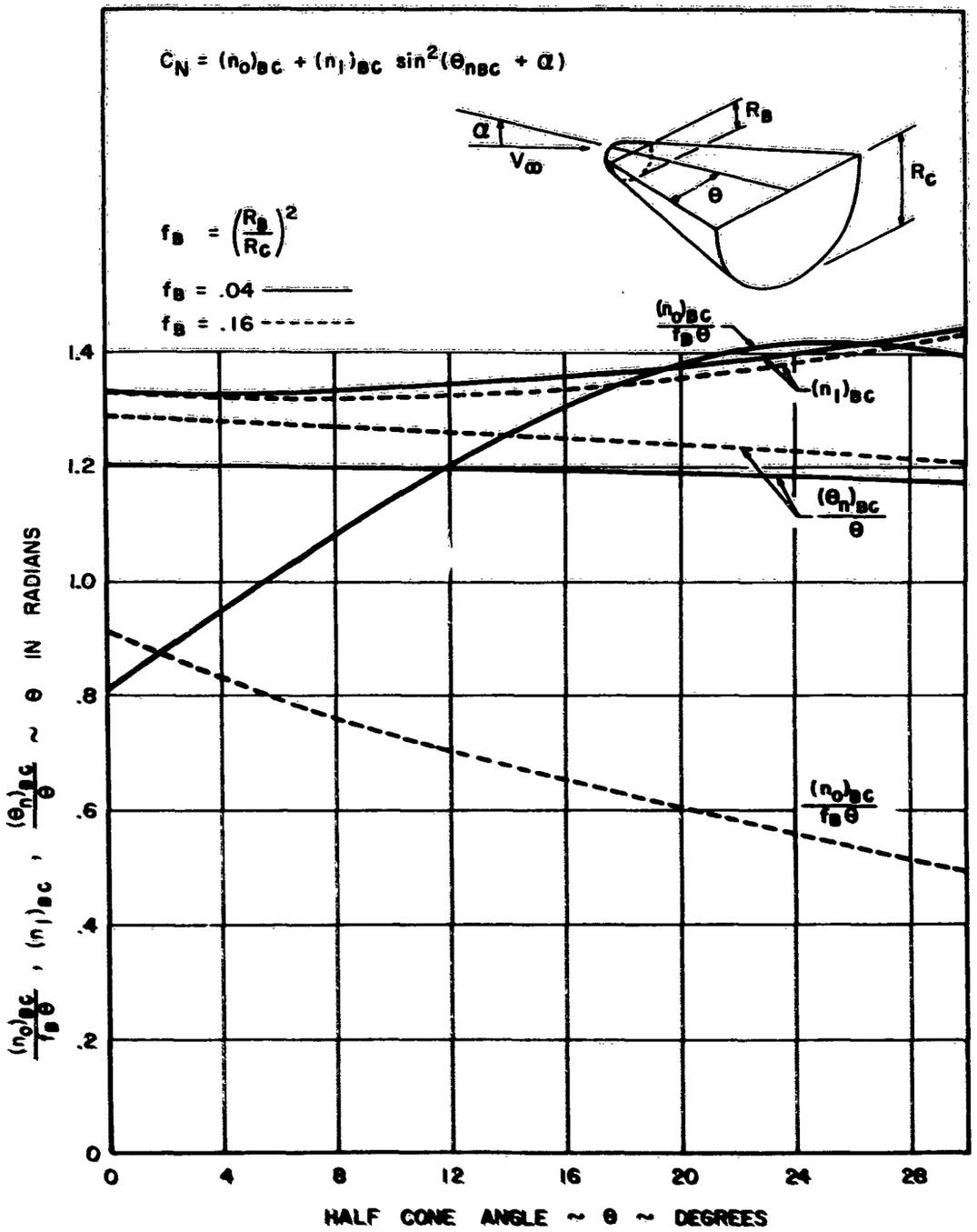

FIGURE 14. NEWTONIAN CONSTANTS FOR A BLUNT CIRCULAR HALF CONE NORMAL FORCE COEFFICIENT

CONDITIONS: $\alpha \geq -\theta$, $\beta = 0$, $\phi = 0$

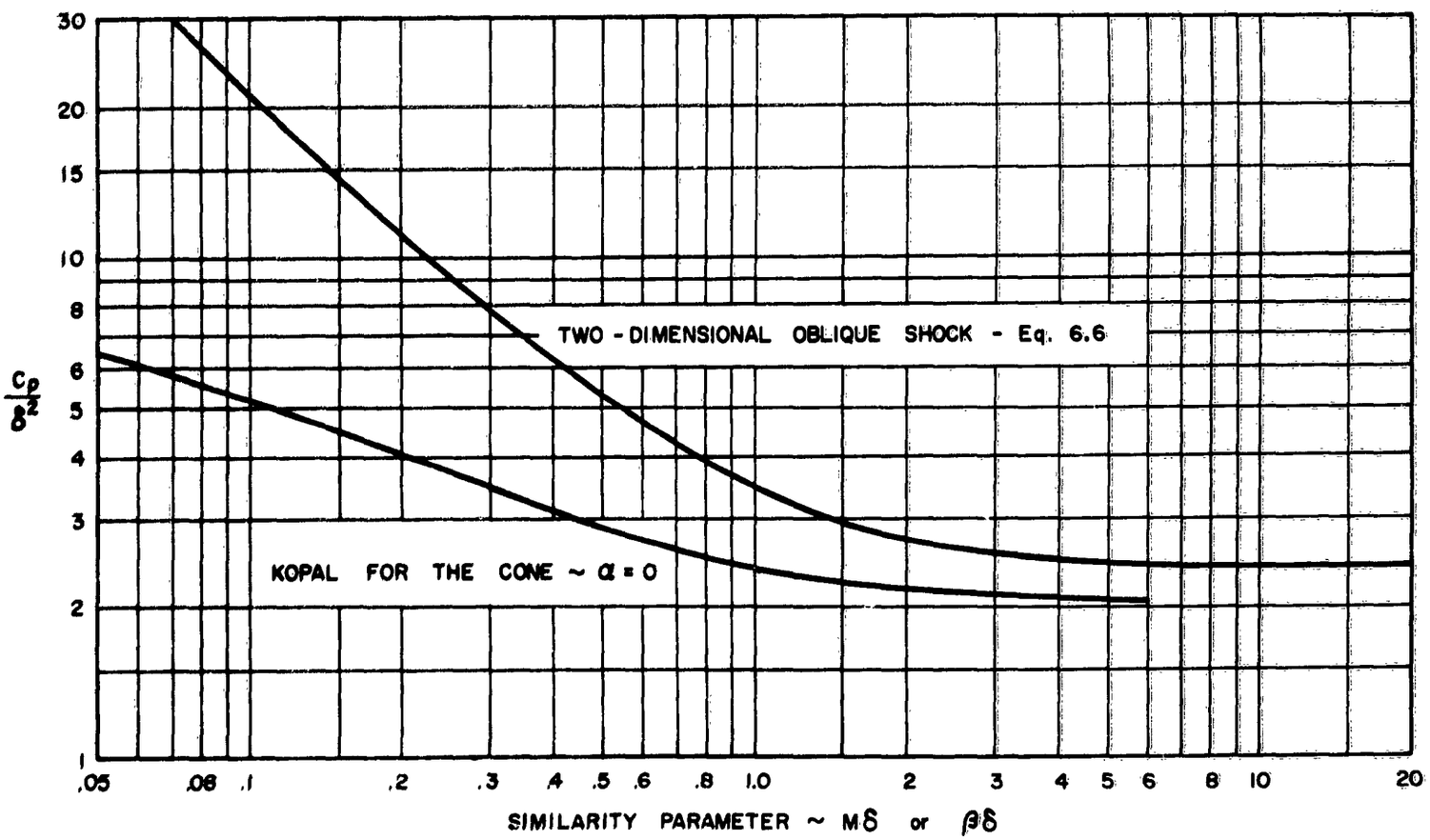

FIGURE 15, TWO AND THREE DIMENSIONAL PRESSURE RELATIONSHIPS AT HYPERSONIC VELOCITIES

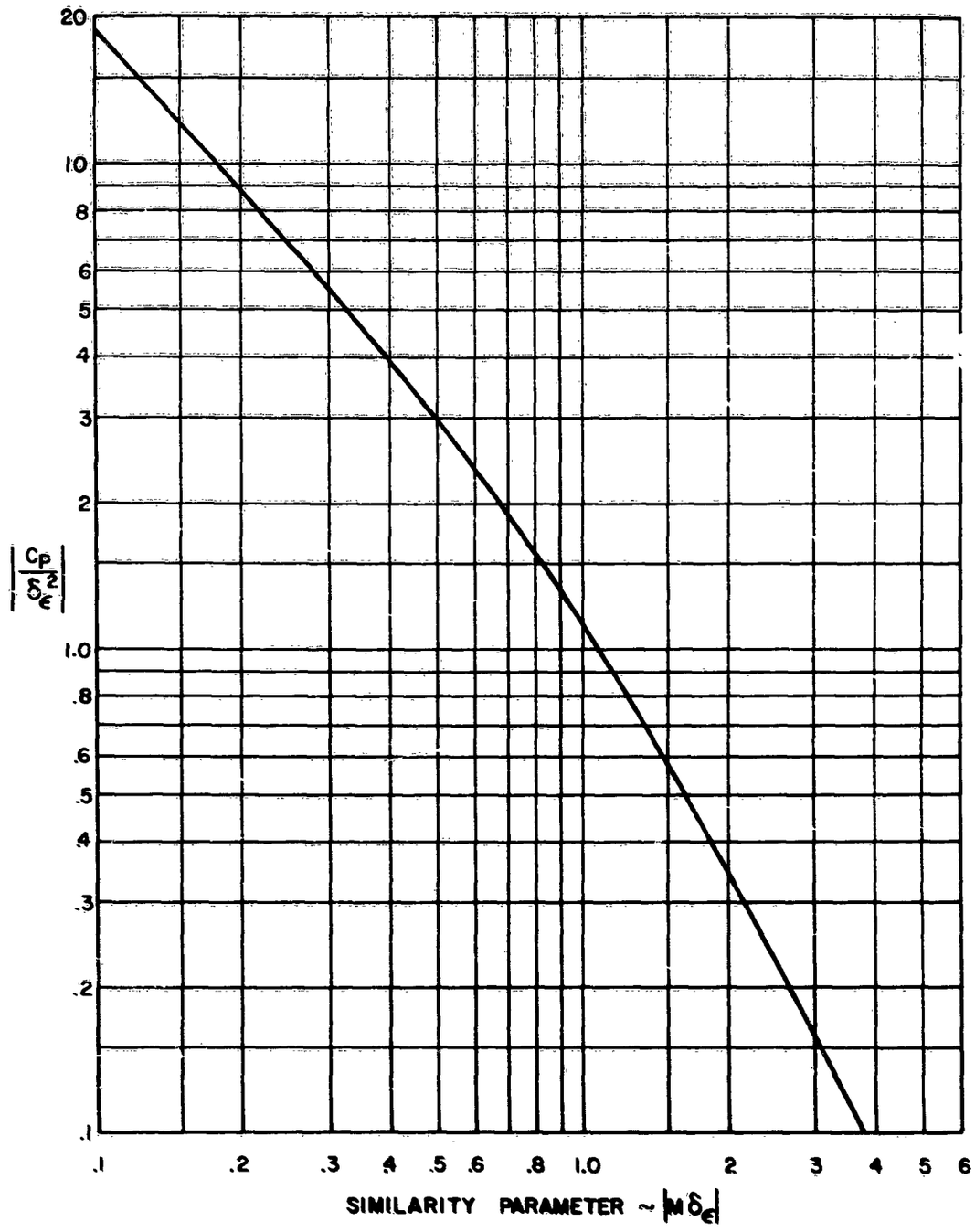

FIGURE 16. PRESSURES DUE TO PRANDTL-MEYER EXPANSION AT HYPERSONIC VELOCITIES.